

# K-BAND PROPERTIES OF GALAXY CLUSTERS AND GROUPS: BRIGHTEST CLUSTER GALAXIES AND INTRACLUSTER LIGHT

YEN-TING LIN<sup>1</sup> AND JOSEPH J. MOHR<sup>1,2</sup>  
*Submitted to ApJ May 30, 2004, Accepted August 30, 2004*

## ABSTRACT

We investigate the near-infrared  $K$ -band properties of the brightest cluster galaxies (BCGs) in a sample of 93 X-ray galaxy clusters and groups, using data from the Two Micron All Sky Survey. Our cluster sample spans a factor of 70 in mass, making it sensitive to any cluster mass related trends. We derive the cumulative radial distribution for the BCGs in the ensemble, and find that 70% of the BCGs are centered in the cluster to within 5% of the virial radius  $r_{200}$ ; this quantifies earlier findings that BCG position coincides with the cluster center as defined by the X-ray emission peak. We study the correlations between the luminosity of the BCGs ( $L_b$ ) and the mass and the luminosity of the host clusters, finding that BCGs in more massive clusters are more luminous than their counterparts in less massive systems, and that the BCGs become less important in the overall cluster light ( $L_{200}$ ) as cluster mass increases. By examining a large sample of optically-selected groups we find that these correlations hold for galactic systems less massive than our clusters ( $< 3 \times 10^{13} M_\odot$ ). From the differences between luminosity functions in high and low mass clusters, we argue that BCGs grow in luminosity mainly by merging with other luminous galaxies as the host clusters grow hierarchically; the decreasing BCG luminosity fraction ( $L_b/L_{200}$ ) with cluster mass indicates that the rate of luminosity growth in BCGs is slow compared to the rate at which clusters acquire galaxy light from the field or other merging clusters.

Utilizing the observed correlation between the cluster luminosity and mass and a merger tree model for cluster formation, we estimate that the amount of intracluster light (ICL) increases with cluster mass; our calculations suggest that in  $10^{15} M_\odot$  clusters more than 50% of total stellar mass is in ICL, making the role of ICL very important in the evolution and thermodynamic history of clusters. The cluster baryon fraction accounting for the ICL is in good agreement with the value derived from Cosmic Microwave Background observations. The inclusion of ICL reduces the discrepancy between the observed cluster cold baryon fraction and that found in hydrodynamical simulations. Based on the observed iron abundance in the intracluster medium, we find that the ICL predicted by our model, together with the observed galaxy light, match the iron mass-to-light ratio expected from simple stellar population models, provided the Salpeter initial mass function is adopted. The ICL also makes it easier to produce the “iron excess” found in the central regions of cool-core clusters.

*Subject headings:* cosmology: observation – galaxies: clusters: general – galaxies: elliptical and lenticular, cD – infrared: galaxies

## 1. INTRODUCTION

The most luminous cluster galaxies (hereafter referred to as brightest cluster galaxies, BCGs) are a unique class of objects. They are ultra-luminous ( $\sim 10 L_*$ , where  $L_*$  is the characteristic luminosity in the galaxy luminosity function; e.g. Schombert 1986) and huge in spatial extent (effective radius  $\sim 30$  kpc; e.g. Schneider et al. 1983b; Schombert 1986; Tonry 1987; Gonzalez et al. 2000, 2004). They tend to lie very close to peaks of the cluster X-ray emission (Jones & Forman 1984; Beers & Tonry 1986; Rhee & Latour 1991, also §2), and in velocity space they sit near the cluster rest frame (e.g. Quintana & Lawrie 1982; Zabludoff et al. 1990; Oegerle & Hill 2001); the implication is that BCGs are located at the minimum in the cluster potential well. Some of the BCGs show multiple nuclei (e.g. Schneider et al. 1983b; Hoessel & Schneider 1985; Lauer 1988) and excess populations of globular clusters compared to normal early type galaxies. (e.g. Harris et al. 1998). Furthermore, correlations between the BCG luminosity and various host cluster properties have been found (e.g. Oemler 1976; Schombert 1987; Edge 1991; Brough

et al. 2002). All these properties indicate they may have a quite unusual formation history compared to other elliptical galaxies.

There are generally three different models proposed for BCG formation: (1) Galactic cannibalism– massive galaxies gradually sink to the center of a cluster because of dynamical friction, and the first galaxy arriving at the center grows in luminosity and mass by merging with latecomers (e.g. Ostriker & Tremaine 1975; Hausman & Ostriker 1978). (2) Cooling flow– stars formed out of the central cooling flow in clusters (e.g. Cowie & Binney 1977). (3) Rapid galactic merger during cluster collapse– BCGs formed from mergers between several galaxies that take place in groups or low mass clusters (Merritt 1985; Dubinski 1998). In this paper we use observed properties of a large sample of BCGs to examine their formation history.

Many of the first ranked galaxies have a large, diffuse envelope around them (the “cD” galaxies; e.g. Tonry 1987; Schombert 1988). The facts that cD galaxies are only found in clusters or local dense structures (Beers & Geller 1983) and that there exist weak correlations be-

<sup>1</sup> Department of Astronomy, University of Illinois, Urbana, IL 61801; ylin2@astro.uiuc.edu

<sup>2</sup> Department of Physics, University of Illinois, Urbana, IL 61801; jmohr@uiuc.edu

tween envelope luminosity and some cluster global properties (Schombert 1988) argue strongly that the formation of the envelopes must be closely connected to the cluster environment.

Due to the dynamical processes such as the mean field tidal stripping (e.g. Merritt 1984) and the cumulative effects of impulsive encounters between galaxies or cluster substructures (“galaxy harassment”, Moore et al. 1996), it is possible that stars may be stripped from galaxies and orbit in intracluster space (which we refer to as the intracluster stellar population or intracluster light, ICL). The investigation of diffuse light in intracluster space has a long history, first based on photographic plates (Zwicky 1951; Welch & Sastry 1971; Oemler 1976; Thuan & Kormendy 1977, only to name a few). Over the past 10 years, there have been many observational studies of the ICL made with CCDs; these include studies of tidal features (e.g. Gregg & West 1998; Trentham & Mobasher 1998; Calcáneo-Roldán et al. 2000), planetary nebulae (e.g. Arnaboldi et al. 2002; Feldmeier et al. 2003a), globular clusters (e.g. Jordán et al. 2003), red giant stars (Ferguson et al. 1998; Durrell et al. 2002) and intracluster supernovae (Gal-Yam et al. 2003). Despite this wealth of data, the amount of ICL is very hard to estimate; the fraction of total cluster light that is in ICL ranges from less than 20% to more than 50% (this may partially reflect a dependence of ICL fraction on cluster mass; see discussion in §4). We note that a complicating factor in estimating the amount of the ICL is the possible connection between the cD envelope and the ICL (Uson et al. 1991). Galactic haloes stripped from their parent galaxies may exist in the intracluster space in the form of a cD envelope (e.g. Richstone 1976; Malumuth & Richstone 1984). In this paper we adopt the view that the cD envelope and the ICL are one and the same, and thus do not attempt to make a distinction between the two (see §§2.2 & 4.1 for further discussions).

This paper is the third in a series in which we systematically study the near-IR (NIR) properties of galaxy clusters. In Lin et al. (2003, hereafter paper I) we develop basic tools for studying the correlation between total galaxy  $K_s$ -band luminosity and cluster binding mass ( $L$ - $M$  relation). In Lin et al. (2004, paper II hereafter) we show the tight  $L$ - $M$  relation in a sample of 93 nearby clusters, using the data from the Two Micron All-Sky Survey (2MASS, Jarrett et al. 2000). We find that the total number of galaxies brighter than a luminosity cutoff is also well correlated with the cluster mass ( $N$ - $M$  relation), and the slope of the  $N$ - $M$  correlation suggests that more massive clusters have smaller mean galaxy number per unit mass, compared to the low mass clusters. The implication is that galaxies are destroyed or stripped and lose light as the process of hierarchical structure formation proceeds toward higher mass scales. In the present paper we aim to study the correlation between the BCG luminosity and cluster mass, thus providing some constraints on BCG formation scenarios, and investigate the amount of ICL that may be present. This will allow us to probe the total cluster stellar population. Due to the depth of the 2MASS, it is not possible to directly measure the amount of ICL; instead we estimate it from simple models that utilize the  $L$ - $M$  relation, the BCG light-cluster mass relation and models of hierarchical structure formation.

The plan of the paper is follows: we describe in §2 our cluster sample, the BCG selection criteria, and the photometry we use for BCG luminosity. Our analysis of BCG properties is presented in §3, where we study the correlation between the cluster mass and the BCG luminosity, and the BCG-to-total galaxy luminosity fraction as a function of cluster mass (§3.1). We discuss constraints on BCG formation scenarios (§3.2) and probe the properties of the second and third ranked galaxies (§3.3). In §4 we model the amount of ICL that may be present in clusters, and use it to examine the enrichment of the intracluster medium. Finally we discuss and summarize our results in §5 & §6, respectively.

Throughout the paper we assume the density parameters for the matter and the cosmological constant to be  $\Omega_M = 0.3$ ,  $\Omega_\Lambda = 0.7$ , respectively, and the Hubble parameter to be  $H_0 = 70 h_{70} \text{ km s}^{-1} \text{ Mpc}^{-1}$ .

## 2. ANALYSIS OVERVIEW

In this section we discuss our cluster sample, the BCG selection, the method we use to estimate total cluster luminosity, and the photometry in the 2MASS catalog that we adopt to obtain BCG luminosity. We further test how reliable the chosen photometry is in representing the total galaxy light.

### 2.1. Cluster Sample and Total $K$ -band Luminosity

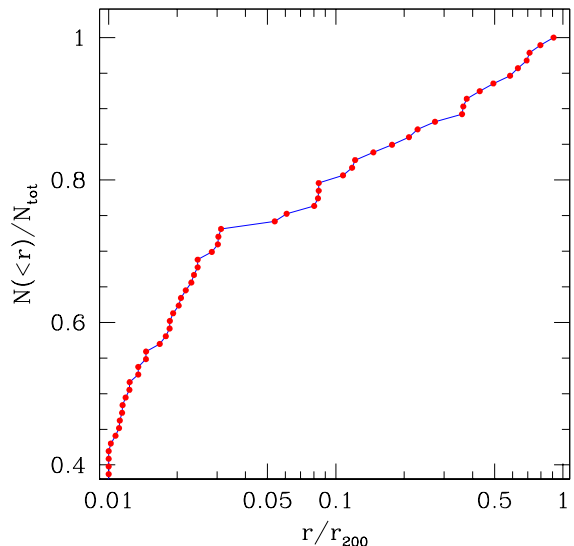


FIG. 1.— Cumulative projected radial distribution of the BCGs. The distance is normalized to the virial radius ( $r_{200}$ ) of each cluster. The number of galaxies located within a given distance is normalized to the total BCG number  $N_{tot} = 93$ . Notice that the BCGs located within 1% of the virial radius are shown to be at  $r/r_{200} = 0.01$ . Note that 75% of the BCGs are located within  $0.06r_{200}$ .

Our cluster sample is built from several X-ray cluster catalogs; please refer to §2 of paper II for the catalog references and a more detailed explanation of our analysis. Here we give a brief account of our procedures. Due to the depth of the 2MASS, we study clusters only out to  $z \leq 0.09$ ; we restrict the clusters to lie above the Galactic plane ( $|b| > 10^\circ$ ). All our clusters have X-ray emission-weighted mean temperature  $T_X$  measurements, from which we estimate the virial radius  $r_{200}$ , within which

TABLE 1  
BCG DATA

Cluster Name	$z$	$T_X$ (keV)	BCG Name <sup>†</sup>	$L_b^{iso\#}$ $10^{11} L_\odot$	$L_b^{ext\#}$ $10^{11} L_\odot$	Cluster Name	$z$	$T_X$ (keV)	BCG Name <sup>†</sup>	$L_b^{iso\#}$ $10^{11} L_\odot$	$L_b^{ext\#}$ $10^{11} L_\odot$
a2319	0.0557	11.8	19211004 + 4356443	9.41 ± 0.50	11.37 ± 0.64	a3562	0.0499	3.80	13320334 + 3146430	5.92 ± 0.33	5.78 ± 0.28
trian	0.0510	9.50	16381810 + 6421367	17.50 ± 0.89	18.87 ± 1.25	a2670	0.0762	3.73	23541371 + 1025084	9.78 ± 0.72	12.31 ± 1.08
a2029	0.0773	8.70	15105610 + 0544416	21.27 ± 1.20	21.33 ± 1.04	a2657	0.0404	3.70	23443040 + 0915499	3.00 ± 0.17	2.91 ± 0.14
a2142	0.0899	8.68	15582002 + 2714000	6.06 ± 0.57	6.67 ± 0.63	a1142	0.0349	3.7	11005745 + 1030197	5.09 ± 0.22	4.70 ± 0.19
a0754	0.0542	8.50	09083238 + 0937470	8.35 ± 0.45	8.41 ± 0.40	a2634	0.0314	3.70	23382938 + 2701526	8.09 ± 0.25	7.99 ± 0.23
a1656	0.0232	8.21	13008009 + 2758372	10.10 ± 0.19	9.56 ± 0.17	2a0335	0.0349	3.64	03384056 + 0958119	5.82 ± 0.26	6.75 ± 0.32
a2256	0.0601	7.51	17042724 + 7838260	7.59 ± 0.51	7.77 ± 0.46	a3526	0.0114	3.54	12484927 + 4118399	8.05 ± 0.13	7.75 ± 0.17
a3667	0.0560	7.00	20122726 + 5649363	9.46 ± 0.54	9.69 ± 0.48	a1367	0.0216	3.50	11440217 + 1956593	4.78 ± 0.12	4.48 ± 0.10
a2255	0.0806	6.87	17122875 + 6403385	6.43 ± 0.47	7.03 ± 0.54	mkw03s	0.0434	3.5	15215187 + 0742319	3.34 ± 0.20	3.51 ± 0.20
a0478	0.0881	6.84	04132526 + 1027551	8.61 ± 0.44	10.81 ± 0.65	a1736	0.0458	3.50	13272804 + 2719288	9.84 ± 0.40	9.63 ± 0.35
a1650	0.0845	6.70	12584149 + 0145410	5.35 ± 0.49	5.74 ± 0.55	hcg094	0.0417	3.45	23171357 + 1842295	10.63 ± 0.41	10.31 ± 0.41
a0644	0.0704	6.59	08172559 + 0730455	5.25 ± 0.47	7.28 ± 0.90	a2589	0.0416	3.38	23235741 + 1646379	6.35 ± 0.36	7.04 ± 0.40
a0426	0.0183	6.33	03194823 + 4130420	7.54 ± 0.14	8.17 ± 0.29	mkw08	0.0270	3.29	14404287 + 0327555	4.64 ± 0.21	4.70 ± 0.19
a1651	0.0860	6.30	12592251 + 0411460	8.90 ± 0.70	10.82 ± 0.96	a4038	0.0283	3.15	23474504 + 2808265	4.07 ± 0.20	4.82 ± 0.27
a3266	0.0594	6.20	04311330 + 6127114	12.23 ± 0.65	14.22 ± 0.83	a1060	0.0114	3.10	10364282 + 2731420	2.89 ± 0.06	3.16 ± 0.11
a0085	0.0551	6.10	00415052 + 0918109	11.53 ± 0.53	11.24 ± 0.46	a2052	0.0348	3.10	15164448 + 0701180	6.59 ± 0.31	7.52 ± 0.38
a2420	0.0846	6.0	22101878 + 1210141	8.89 ± 0.75	12.74 ± 1.48	a0548e	0.0395	3.10	05483835 + 2528404	4.99 ± 0.28	5.33 ± 0.28
a0119	0.0440	5.80	00561610 + 0115197	8.45 ± 0.39	8.55 ± 0.38	a2593	0.0433	3.1	23242006 + 1438492	6.58 ± 0.40	7.48 ± 0.45
a3391	0.0531	5.70	06262045 + 5341358	16.27 ± 0.61	15.93 ± 0.54	as039	0.0288	3.04	05163713 + 0626526	5.07 ± 0.15	4.22 ± 0.31
a3558	0.0480	5.70	13275688 + 3129437	13.50 ± 0.63	14.95 ± 0.72	as1101	0.0580	3.00	23135863 + 4243393	5.42 ± 0.38	7.80 ± 0.70
a3158	0.0590	5.50	03425295 + 5337526	6.72 ± 0.47	9.14 ± 0.83	a0779	0.0230	2.97	09194687 + 3344594	7.69 ± 0.18	7.21 ± 0.15
a1991	0.0590	5.4	14543146 + 1838325	5.73 ± 0.40	6.85 ± 0.48	awm4	0.0326	2.92	16045670 + 2355583	7.11 ± 0.24	7.05 ± 0.22
a2065	0.0726	5.37	15215562 + 2724530	3.81 ± 0.28	4.93 ± 0.29	exo0422	0.0390	2.90	04255133 + 0833389	5.14 ± 0.25	5.13 ± 0.21
a1795	0.0631	5.34	13485251 + 2635348	6.40 ± 0.37	9.08 ± 0.68	a2626	0.0553	2.9	23363057 + 2108498	7.48 ± 0.47	8.24 ± 0.46
a3822	0.0760	5.12	21550019 + 5739278	6.62 ± 0.45	6.86 ± 0.47	zw1615	0.0302	2.9	16174059 + 3500154	2.75 ± 0.10	2.77 ± 0.10
a2734	0.0620	5.07	00112166 + 2851158	6.23 ± 0.42	7.70 ± 0.55	mkw09	0.0397	2.66	15323201 + 0440516	4.06 ± 0.23	4.32 ± 0.23
a3395sw	0.0510	5.00	06273625 + 5426577	6.62 ± 0.43	7.77 ± 0.47	a0194	0.0180	2.63	01260057 + 0120424	6.49 ± 0.13	5.41 ± 0.05
a0376	0.0484	5.0	02460391 + 3654188	5.62 ± 0.33	6.60 ± 0.41	a0168	0.0450	2.6	01145760 + 0025510	5.26 ± 0.26	5.54 ± 0.26
a1314	0.0335	5.0	11344932 + 4904388	4.87 ± 0.15	5.05 ± 0.15	a0400	0.0240	2.43	02574155 + 0601371	5.61 ± 0.27	6.38 ± 0.27
a2147	0.0351	4.91	16021984 + 1620462	4.70 ± 0.17	4.71 ± 0.16	a0262	0.0161	2.41	01524648 + 3609065	4.25 ± 0.11	4.08 ± 0.10
a3112	0.0750	4.70	03175766 + 4414175	11.15 ± 0.68	14.40 ± 0.93	a2151	0.0369	2.40	16043575 + 1743172	5.62 ± 0.20	5.07 ± 0.19
a1644	0.0474	4.70	12571157 + 1724344	11.35 ± 0.61	12.67 ± 0.69	mkw04s	0.0283	2.13	12063891 + 2810272	7.53 ± 0.17	7.23 ± 0.15
a1909	0.0303	4.50	16283827 + 3933049	8.45 ± 0.28	8.05 ± 0.24	a3389	0.0265	2.1	06222206 + 6456025	5.64 ± 0.20	5.32 ± 0.17
a2107	0.0421	4.31	15393904 + 2146579	7.78 ± 0.34	7.91 ± 0.31	ivew038	0.0170	2.07	01072493 + 3224452	5.30 ± 0.11	4.92 ± 0.10
a0193	0.0486	4.2	01250764 + 0841576	7.77 ± 0.31	8.21 ± 0.34	as0636	0.0116	2.06	10302648 + 3521343	3.49 ± 0.07	3.15 ± 0.06
a2063	0.0355	4.10	15230530 + 0836330	4.34 ± 0.24	4.77 ± 0.27	a3581	0.0230	1.83	14072978 + 2701043	3.41 ± 0.12	3.29 ± 0.10
a4059	0.0475	4.10	23570068 + 3443531	10.41 ± 0.50	10.75 ± 0.50	mkw04	0.0200	1.71	12042705 + 0153456	7.13 ± 0.21	6.65 ± 0.18
a1767	0.0701	4.1	13360827 + 5912229	8.67 ± 0.56	11.29 ± 0.86	ngc6338	0.0282	1.69	17152291 + 5724404	6.07 ± 0.18	5.70 ± 0.15
a0576	0.0389	4.02	07273023 + 5545416	6.53 ± 0.26	9.45 ± 0.70	a0076	0.0405	1.5	00392632 + 0644028	6.87 ± 0.24	7.17 ± 0.26
a3376	0.0456	4.00	06004111 + 4002398	5.81 ± 0.34	5.96 ± 0.31	ngc6329	0.0276	1.45	17141500 + 4341050	4.00 ± 0.13	3.61 ± 0.10
a0133	0.0569	3.97	10124177 + 2152557	7.76 ± 0.47	8.08 ± 0.42	as0805	0.0140	1.4	18471814 + 6319521	4.92 ± 0.11	4.52 ± 0.10
a0496	0.0328	3.91	04333784 + 1315430	7.00 ± 0.28	7.35 ± 0.28	ngc0507	0.0165	1.26	01233995 + 3315222	5.62 ± 0.12	5.45 ± 0.12
a1185	0.0325	3.9	11103843 + 2846038	4.50 ± 0.14	4.49 ± 0.13	ngc2563	0.0163	1.06	08203567 + 2104042	3.04 ± 0.06	2.76 ± 0.05
awm7	0.0172	3.90	02542739 + 4134467	6.79 ± 0.14	6.39 ± 0.15	wp23	0.0087	1.0	13165848 + 1638054	2.87 ± 0.05	2.95 ± 0.10
a2440	0.0904	3.88	22235694 + 0134593	6.24 ± 0.41	6.21 ± 0.42	ic4296	0.0133	0.95	13363905 + 3357572	8.13 ± 0.16	7.42 ± 0.14
a3560	0.0489	3.87	13314673 + 3253401	4.88 ± 0.28	5.44 ± 0.34	hcg062	0.0137	0.87	12530567 + 0912141	2.99 ± 0.09	2.77 ± 0.08
a0780	0.0538	3.80	09180565 + 1205439	5.22 ± 0.35	5.11 ± 0.30						

<sup>†</sup>The 2MASS designation, where the prefix 2MASXJ is omitted.

<sup>‡</sup> $L_b^{iso}$  is obtained by subtracting 0.2 mag from the isophotal magnitudes;  $L_b^{ext}$  is given by the extrapolated total magnitudes. These are extinction and  $k$ -corrected luminosities.

the enclosed mean overdensity is 200 times the critical density of the universe,  $\rho_c$ . The cluster masses range from  $3 \times 10^{13} h_{70}^{-1} M_\odot$  to  $2 \times 10^{15} h_{70}^{-1} M_\odot$ , spanning approximately a factor of 70 in virial mass. We define the cluster center as the peak of the X-ray emission, either from the cluster catalogs or from archival *ROSAT* images. The cluster redshift is from the catalogs or NED/SIMBAD. For each cluster, we build a galaxy catalog from the 2MASS extended source catalog for galaxies brighter than the 2MASS completeness limit  $K_s = 13.5$  mag (hereafter we denote  $K_s$  by  $K$  for simplicity) that lie within the virial radius.

Within each galaxy catalog, we sort the galaxies according to their apparent magnitudes, and search for redshift information from the NED for the bright galaxies. Redshift measurements are available for most of the galaxies. We consider galaxies with recession velocity within  $v_c \pm 3\sigma_v$  as cluster members, where  $v_c$  and  $\sigma_v$  are cluster recession velocity and velocity dispersion, respectively, which are collected from the literature (Struble & Rood 1999; Wu et al. 1999). We do not choose BCGs based on their morphology.

We list in Table 1 the BCGs in our sample. The table contains the cluster name, cluster redshift and X-ray temperature, BCG name (under the 2MASS designation), BCG luminosities derived from 2MASS isophotal and extrapolated total photometries, respectively (see §2.2).

There is one cluster whose BCG could not be unambiguously determined, because no redshift measurement is available (Exo 0422-086); we assign the brightest galaxy

as the BCG, as it lies very close to the cluster center (the projected distance is  $0.007 r_{200}$ ). Removing this system from the sample does not change our results.

In Fig 1 we show the cumulative radial distribution of the BCGs, with radial distance normalized to the virial radius of the host clusters. The majority of the galaxies that we assign as BCGs is located at the center of the cluster potential, as traced by the X-ray emission. For example, about 45% of the BCGs are located within 1% of the virial radius, and 90% within  $0.38 r_{200}$ . It has long been recognized that BCGs lie very close to the cluster center (e.g. Jones & Forman 1984; Beers & Tonry 1986; Rhee & Latour 1991; Postman & Lauer 1995; Lazzati & Chincarini 1998); what is new from our analysis are the large cluster sample size and the adoption of the cluster virial radius as a fundamental scale. An important implication is that, in the absence of X-ray images or detailed kinematic information about the galaxies, the BCG position can serve as a good proxy for the cluster center.

Except for those clusters undergoing major mergers, in which case BCGs may be far from the minimum of the cluster potential, we do not expect BCGs to lie far from the X-ray peaks. Within this context, the figure also allows us to estimate the accuracy of our BCG selection. In cases of merging, the galaxy we identify as the BCG may well be a chance interloper. From the figure we see that  $\sim 8\%$  of our BCGs lie at  $r > 0.5 r_{200}$ ; indeed, most of the second-ranked galaxies of these clusters lie at  $r < 0.1 r_{200}$ . This implies a  $\lesssim 10\%$  contamination rate from non-BCGs

in the BCG luminosity–cluster mass correlations (§3), and this may be a source of the scatter. We note, however, restricting the BCGs to lie well within the cluster virial radius (e.g.  $r_{500} \approx 0.6r_{200}$ , within which the mean density is  $500\rho_c$ ) has very little effect on the cluster  $L$ – $M$  relation, or the BCG light fraction (see §3.1 below).

Given the high frequency of clusters exhibiting X-ray evidence of mergers (50 – 70%, as inferred from the centroid variations, e.g. Mohr et al. 1995), the preponderance of centrally located BCGs in this sample (Fig 1) seems rather surprising. This may suggest that the timescale for the BCG to sink to the cluster potential minimum is short compared to the relaxation timescale of the intracluster gas. Alternatively, the scale of merger required to perturb the X-ray properties of the cluster could be smaller than the scale of the merger required to perturb the BCG from the cluster center.

To estimate the total cluster light for each cluster, we calculate the total observed number and luminosity from member galaxies (excluding the BCG); corrections for background/foreground galaxies are estimated statistically. From the total number and luminosity we solve for the cluster luminosity function (LF)  $\phi(L)$ . Specifically, with a fixed faint-end slope  $\alpha = -1.1$ , we solve for the characteristic luminosity  $L_*$  and density  $\phi_*$  in the functional form proposed by Schechter (1976). We note the choice of  $\alpha$  is consistent with the “stacked” luminosity function formed from all our 93 clusters (see §3.2 in paper II). The total luminosity from galaxies, which are within the virial region and are brighter than a minimum luminosity  $L_{min}$ , is then  $L_{200} = \int_{L_{min}}^{\infty} \phi(L)LdL + L_b$ , where  $L_b$  is the BCG luminosity, and we choose  $L_{min}$  that corresponds to  $M_{min} = -21$  mag. Our approach is described in more detail in §2 of paper I.

## 2.2. 2MASS Photometry of BCGs

We use the  $\mu_K = 20$  mag/arcsec<sup>2</sup> isophotal elliptical aperture magnitudes provided by the 2MASS extended source catalog for both the BCGs and other galaxies. The effects of Galactic extinction and  $k$ -correction are included. We use the value of the extinction coefficient provided by the NED at the cluster center, and adopt a  $k$ -correction of the form  $k(z) = -6 \log(1+z)$  (Kochanek et al. 2001). More importantly, we make a correction of 0.2 mag to convert to the “total” magnitudes, following Kochanek et al. (2001). This value is inferred by comparing 2MASS (second incremental release) isophotal magnitudes with deeper photometry (Kochanek et al. 2001), and is consistent with the estimate that the isophotal magnitudes capture 80 – 90% of the integrated flux for normal galaxies<sup>3</sup>. However, given the peculiar properties of the BCGs (especially those that belong to the cD class), we do not expect the simple correction for normal galaxies to apply to BCGs. Below we use published BCG photometry to investigate how well this naive correction works in recovering the BCG “total” light. We emphasize here that we do *not* attempt to *measure* the total BCG light, but are mostly concerned with the correlations between an objective measure of BCG light and cluster mass (§3).

Bearing our objective in mind, it is crucial that the isophotal photometry we choose does not introduce any

cluster mass related systematics. To be specific, we have to understand if there is any (cluster) mass-dependent structural variation in the BCGs that will affect the isophotal photometry. To this end, we gather from the literature observed surface brightness profiles for 49 BCGs whose host clusters have measured X-ray temperatures (primarily from Graham et al. 1996, with additional measurements from Gonzalez et al. 2000; Fasano et al. 2002; Graham 2002; below they are referred to as the known profile BCG sample). With appropriate colors  $R - K = 2.6$ ,  $r - K = 2.5$ ,  $I - K = 2.0$  &  $B - K = 4.2$  for early type galaxies, we transform the measured profiles into the  $K$ -band, and calculate the differences between the  $\mu_K = 20$  mag/arcsec<sup>2</sup> magnitudes and those corresponding to  $\mu_K = 20.9$  &  $21.5$  mag/arcsec<sup>2</sup>. We caution that because the completeness limit of Graham et al. (1996) sample is at  $\mu_R = 23.5$  mag/arcsec<sup>2</sup>, some of the magnitude differences shown in Fig 2 are *extrapolations*. The resulting differences depend on the surface brightness profiles of the galaxies, as well as the surface brightness at which the magnitudes are obtained. From the figure it is seen that on average the magnitude differences are  $\overline{\Delta m}(\mu_{20} - \mu_{20.9}) = 0.26$ ,  $\overline{\Delta m}(\mu_{20} - \mu_{21.5}) = 0.43$ . Furthermore, we notice that the BCG surface brightness profile are typically described by either a Sersic profile or a power-law (Graham et al. 1996). The average magnitude differences for those galaxies best-fit by Sersic profiles (36 galaxies) are 0.21 & 0.36 mag at different surface brightness, while for the 13 galaxies best described by power-laws they are 0.38 & 0.63. The larger magnitude difference for the latter is expected, because of the flatness of the profiles. This exercise also indicates that the surface brightness profiles must steepen at larger radii (or fainter surface brightness) or the “total” light of the BCGs would be ill-defined.

Interestingly, we note the differences do not show any obvious trend with either cluster redshift or temperature (i.e. mass). As the 49 BCGs span wide ranges in the best-fit profile parameter space (c.f. Graham et al. 1996) and their host clusters in the  $z - T_X$  space, the results of this test should be representative of nearby BCGs and, therefore, our galaxy sample.

The above test shows that our simple scheme of “correcting” the galaxy magnitudes by subtracting 0.2 mag from the isophotal magnitudes should not introduce any systematic correlation between the BCG light and cluster mass. However, it is also important to see how much light is recovered from this 0.2 mag correction. Apparently this depends on the BCG light profile and the depth desired. 2MASS provides photometries derived from larger apertures, such as Kron and “total” (extrapolated) magnitudes. These are obtained by fitting a Sersic profile in a large area around each galaxy. We choose to use the isophotal magnitudes for the BCGs, as used for other galaxies, for the homogeneity of the analysis, and also to prevent possible contamination from nearby stars or surface brightness fluctuations on the sky.

We examine the differences between the isophotal and the total extrapolated magnitudes for the BCGs, and find that for about 75% of all 93 BCGs the magnitude difference is 0.2 mag, with a scatter of  $\sim 0.1$  mag. This implies a

<sup>3</sup> <http://www.ipac.caltech.edu/2mass/releases/allsky/doc/explsup.html>

0.2 mag correction to the isophotal magnitude gives an accuracy good to  $\sim 10\%$ . Most of the remaining 25% of the BCGs (23 galaxies) belong to clusters at  $0.02 \leq z \leq 0.09$  that have masses  $2 \times 10^{14} M_\odot \leq M_{200} \leq 7.5 \times 10^{14} M_\odot$ . By inspecting the postage stamp images of these galaxies<sup>4</sup>, we find that most of them have nearby bright sources at  $0'.5 - 1'$  around them.

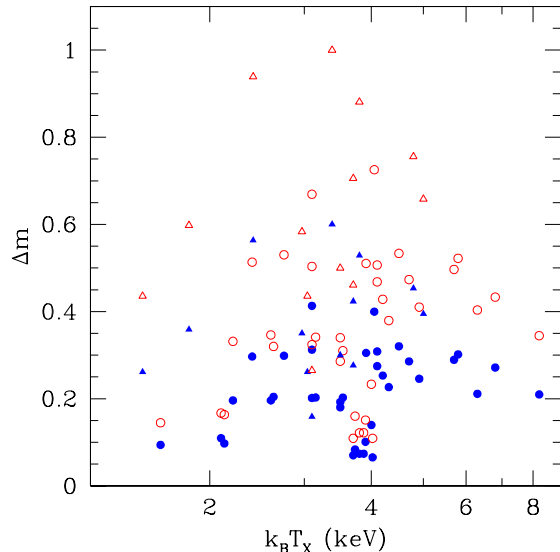


FIG. 2.— Differences in isophotal magnitudes at  $\mu_K = 20$  mag/arcsec<sup>2</sup> and at other surface brightness (solid points: 20.9 mag/arcsec<sup>2</sup>, hollow points: 21.5 mag/arcsec<sup>2</sup>). The circular points indicate the galaxy is best-fit by a Sersic profile, while the triangles represent those best-fit by a power-law surface brightness profile. Notice that there is no apparent trend between the magnitude differences and cluster mass (X-ray temperature).

In addition to possible contamination from nearby sources, cosmic dimming is also a probable cause of the larger difference between the photometries. At greater redshifts the cosmic dimming may affect the isophotal photometry and in turn any correlation between the BCG and cluster mass, as more massive clusters in our sample tend to lie at higher redshifts. We artificially place the galaxies in the known profile BCG sample at different redshifts and evaluate the magnitudes of cosmic dimming. It is found that if the clusters were all at  $z \sim 0.1$ , dimming would cause a change of 0.05 to  $\lesssim 0.2$  mag. Furthermore, we do not see any correlation between the profile shape and the redshift for the BCGs of known profiles. In particular, we note that 7 of the 23 known profile BCGs that lie in our sample of 93 have no apparent systematic differences in their profile parameters compared to the other BCGs of known profiles.

Thus, for the analysis below we estimate the BCG (as well as other cluster galaxies) magnitude as 0.2 mag less than the 2MASS elliptical, isophotal magnitudes.

### 3. CONNECTION BETWEEN BCGS AND HOST CLUSTERS

In paper II we analyze the  $L$ – $M$  relation, the correlation between the total light from all the cluster galaxies and the cluster mass. Let  $L_g$  denote the luminosity from all galaxies except for the BCG; we find that  $L_{200} = L_g + L_b \propto M_{200}^{0.72 \pm 0.04}$ , while  $L_g \propto M_{200}^{0.82 \pm 0.04}$ .

<sup>4</sup> <http://irsa.ipac.caltech.edu/applications/2MASS/PubGalPS/>

This implies that the importance of the BCG contribution to cluster light depends on the cluster mass, and that BCG luminosity is very important in the cluster light budget. By examining any correlations between properties of the BCGs and host clusters, one may be able to place constraints on the formation scenarios of the BCGs and more broadly, the evolution of the clusters.

Below we first study the  $L_b$ – $M_{200}$  correlation in detail, and then discuss the BCG contributions to the total light across a factor of 70 in cluster mass (§3.1). We then use these observations to discuss the BCG formation history (§3.2). Finally we investigate the photometric and kinetic properties of the second- and third-ranked galaxies (hereafter G2 and G3) in a subset of our cluster sample (§3.3).

A word of caution is in order here— although in this section we often refer to  $L_{200}$  as the total light in a system, it actually means the total light in galactic objects. As we argue in §1, the evidence for a stellar population in intracluster space is firm, and the ICL contribution to the total cluster light may not be negligible. Furthermore, we regard stars in extended diffuse envelopes around some BCGs as part of the ICL. We therefore use the notation  $L_{tot}$  to denote light from all known stellar populations in clusters (the BCG and the ICL, and the galaxies) brighter than a luminosity cutoff.

#### 3.1. BCG Luminosity and Cluster Mass

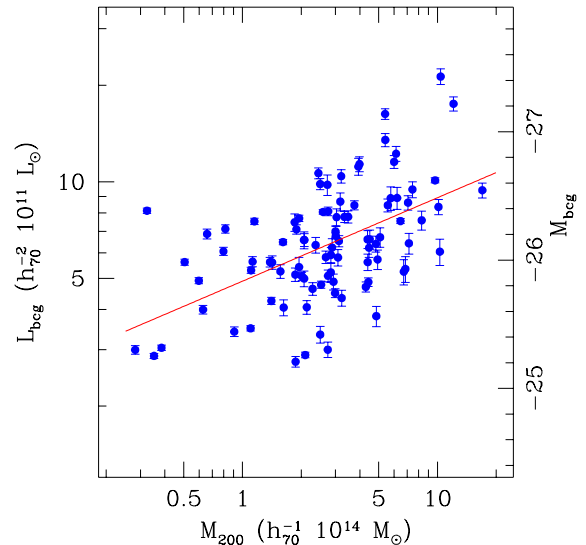


FIG. 3.— The correlation between the BCG luminosity (estimated from the isophotal magnitudes) and the cluster virial mass. On the right axis is shown the corresponding magnitudes. Overall the BCG luminosity scales with cluster mass as  $L_b \propto M_{200}^{0.26 \pm 0.04}$  (the solid line).

BCGs are well-known for the similarity of their luminosity (e.g. Sandage 1972, 1976; Hoessel et al. 1980; Schneider et al. 1983a; Collins & Mann 1998), and there have even been attempts to use them as standard candles in a cosmological context (Postman & Lauer 1995). In Fig 3 we plot the BCG  $K$ -band isophotal magnitudes against the mass of their parent cluster. The BCGs in our sample have a mean magnitude of  $M_K = -26.12 \pm 0.05$  mag, with

a 0.44 mag scatter about the mean. For comparison, the characteristic magnitude of the composite cluster LF for our cluster sample is  $M_{K*} = -24.34$  (paper II).

Considering the vastly different environments in clusters in our sample, it is not surprising that a spread in BCG luminosity is present; however, more interesting is the apparent correlation between  $L_b$  and cluster binding mass. Below the mass scale  $\sim 10^{14} M_\odot$ ,  $L_b$  seems to be rather constant (although see §5.2), however, for systems more massive, there is a trend; a least-square fit to the data for 11 systems with  $M_{200} < 10^{14} M_\odot$  gives

$$\frac{L_b}{10^{11} h_{70}^{-2} L_\odot} = 5.7^{+3.4}_{-2.1} \left( \frac{M_{200}}{10^{14} h_{70}^{-1} M_\odot} \right)^{0.32 \pm 0.30},$$

consistent with a flat distribution; for 82 clusters more massive than  $10^{14} M_\odot$  we have

$$\frac{L_b}{10^{11} h_{70}^{-2} L_\odot} = 4.4 \pm 0.3 \left( \frac{M_{200}}{10^{14} h_{70}^{-1} M_\odot} \right)^{0.33 \pm 0.06}.$$

When fitting the whole BCG sample, we find

$$\frac{L_b}{10^{11} h_{70}^{-2} L_\odot} = 4.9 \pm 0.2 \left( \frac{M_{200}}{10^{14} h_{70}^{-1} M_\odot} \right)^{0.26 \pm 0.04}. \quad (1)$$

The Spearman correlation coefficient is 0.51, with a probability of  $1.5 \times 10^{-7}$  that such correlation happens by chance. The fractional scatter about the fit is 34%.

There have been many attempts to examine how well BCGs correlate with the parent clusters, as this may reveal the connection between the two (e.g. Sandage & Hardy 1973; Sandage 1976; Hoessel et al. 1980; Schneider et al. 1983a; Postman & Lauer 1995; Graham et al. 1996; Collins & Mann 1998; Katayama et al. 2003, among others). Using photographic data, Oemler (1976) shows both  $L_b$  &  $L_{b+env}$  correlate with the total cluster luminosity for a sample of cD galaxies, where  $L_{b+env}$  is the luminosity of the galaxy and the cD envelope associated with it. This result is confirmed later within a much larger sample (Schombert 1987, 1988). The former study also finds correlations between  $L_b$  and total observed galaxy number, cluster velocity dispersion, and X-ray luminosity, although not to a high degree. A joint X-ray and  $K$ -band analysis of 22 clusters finds weak correlation between  $L_b$  and cluster temperature (Edge 1991), which we now know is a good proxy for cluster virial mass. Subsequent studies have confirmed these earlier findings (e.g. Fisher et al. 1995; Brough et al. 2002; De Grandi et al. 2004, and references therein). Our result also agrees qualitatively with the previous investigations, but it is unique in the relatively large sample size and its broad range in mass, the reliable cluster mass estimates (derived from X-ray temperature measurements), the physical quantities being evaluated at fixed overdensities, and the use of  $K$ -band data, which is less sensitive to on-going star formation.

What is less appreciated in previous studies is the BCG luminosity fraction, i.e. the BCG-to-total luminosity ratio. There have been estimates of this fraction for some clusters (e.g. A2029, BCG+envelope,  $\sim 23\%$  in  $R$ -band, Usen et al. 1991; A1651, BCG+halo,  $\sim 36\%$  within 0.7 Mpc, in  $I$ -band, Gonzalez et al. 2000; three massive clusters at  $0.8 < z \lesssim 1.0$ , 10–16% in  $K$ -band, Ellis & Jones 2004). These results show that indeed the BCG contribution to total cluster light is large. With the large sample

and the information on the total light from cluster galaxies, we are in good shape to study the BCG luminosity fraction from groups to massive clusters, which is plotted in Fig 4. We recall that the total luminosity is obtained by summing the contributions from the BCG and from other cluster galaxies, where the latter component is obtained by integrating the LF of individual clusters. We also note that the uncertainty in the “total” BCG light should not affect the overall trend (except for the normalization), because, as shown in the previous section, the magnitude differences between the  $\mu_K = 20$  mag/arcsec<sup>2</sup> isophotal and deeper photometry do not depend on system mass.

As clearly shown in the figure, the BCG light constitutes a very large fraction of total light at group mass scales (40–50%), but becomes less important in the overall luminosity budget progressively, as we move to highest mass clusters ( $\sim 5\%$ ). To be more quantitative, we find in paper II that the light from normal galaxies in clusters grow as  $M_{200}^{0.82 \pm 0.04}$ ; as long as the slope is greater than that of the  $L_b$ – $M$  correlation, a decreasing BCG luminosity fraction is a natural outcome. Clusters appear to gain light faster than BCGs do, which may be the case when a significant number of galaxies are accreted from either the field environments or less massive groups or clusters, while at the same time the rate of BCG growth (e.g. via galactic cannibalism or mergers) remains rather modest. We explore this possibility as well as some BCG formation and evolution scenarios in the next section.

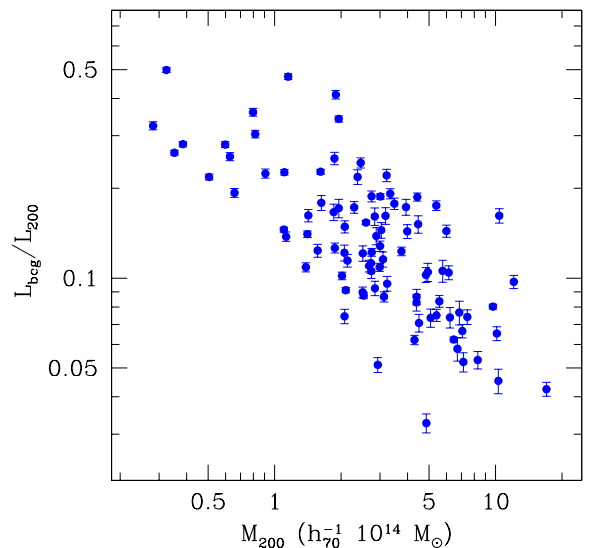


FIG. 4.— The BCG light fraction, defined as the ratio of BCG luminosity-to-total cluster galaxy light (BCG and other galaxies). The comparatively low rate of galaxy mergers with the BCG as groups are merged hierarchically into more massive clusters leads to the decreasing BCG light fraction (see §3.2.2).

### 3.2. Implications for BCG Formation and Evolution

There are several proposals for the formation and evolution of the BCGs, including “galactic cannibalism”, a rapid merger among galaxies during the collapse and virialization of low mass systems, and the cooling flows. In the first scenario, orbital radii of galaxies decrease with time because of dynamical friction, and eventually galaxies merge with the galaxy that first sinks to the bottom of the



gravitational potential. Therefore a central galaxy grows in mass and luminosity as the cluster evolves (Ostriker & Tremaine 1975; Richstone 1976; Hausman & Ostriker 1978; Malumuth & Richstone 1984). This picture has been criticized for requiring unreasonably short dynamical friction timescales, and overpredicts the luminosity gained through mergers over cosmic time (Merritt 1983). Instead, Merritt (1984, 1985) show that the dynamic friction time scale is very long compared to the Hubble time (due to the cluster mean field tidal stripping of subhaloes), and the most likely way of forming a giant central galaxy is by rapid merging at an epoch during the collapse and virialization of groups or low mass clusters. In the third theory, strong star formation activity takes place at cluster centers because of the cooling of gas (e.g. Cowie & Binney 1977; Fabian 1994). The absence of a large color gradient together with the red color of BCGs seem to argue against this possibility, unless the stars formed are biased toward low mass (Edge 1991). Furthermore, recent X-ray observations suggest the ICM in “cool-core” clusters never cools below 1 – 2 keV (e.g. Peterson et al. 2001), and so we can rule out this scenario.

Between the other two scenarios, the rapid merging during low mass cluster collapse seems to be more plausible. A high resolution  $N$ -body simulation which follows the hierarchical build up of a Virgo-like cluster suggests the BCG does form in a relatively short phase early in cluster evolution, through mergers with a few massive galaxies (Dubinski 1998). The alignment between the BCG semimajor axis and the surrounding large-scale structure also seems to support this idea, as the preferred direction for merger or accretion would be along the large scale filaments (West 1994). Furthermore, there is direct observational evidence of mergers involving the brightest members taking place in intermediate and high redshift clusters (Nipoti et al. 2003; Yamada et al. 2002).

Under this scenario, the natural formation sites for (progenitors of) BCGs are low mass systems, because the merger rate is a steeply declining function of the velocity dispersion of a system (Merritt 1985). The subsequent evolution of the BCGs has to explain the existence of the  $L_b$ – $M$  correlation (Fig 3). A simple picture is that BCGs form in groups and become BCGs or other bright galaxies in more massive systems, as hierarchical structure formation continues (Merritt 1985; Edge 1991). After a central dominant galaxy in the merged system is formed, cannibalism can take place, but with a very small luminosity ingestion rate (e.g.  $\sim 2 - 4 L_*$  over a course of 10 Gyrs, Merritt 1985; Lauer 1988; Tremaine 1990). Given that  $L_* \sim 10^{11} L_\odot$  (paper II), this amount seems to be able to account for the mild increase of  $L_b$  from group scales ( $M_{200} \leq 10^{14} M_\odot$ ) to low or intermediate mass clusters ( $M_{200} \leq 5 \times 10^{14} M_\odot$ ),  $\Delta L_b \sim 3 L_*$  (c.f. Fig 3). To produce the more luminous BCGs in more massive clusters, other mechanisms may be needed.

Below we seek plausible scenarios based on the observations presented in the previous section and in paper II. We first compare the luminosity functions of high and low mass clusters and argue that BCGs in massive clusters are likely built from luminous galaxies in progenitors of the host clusters (§3.2.1); then we show that the  $\Lambda$ CDM model supports this scenario and leads to the observed

decreasing BCG light fraction (§3.2.2).

Before we proceed, it is worth mentioning that we have adopted the view that the BCGs in our sample represent a continuous evolution track. BCGs in the present-day high mass clusters may be evolved from low mass cluster BCGs at higher redshifts, which may not be the same as those in the  $z = 0$  low mass clusters. We have neglected this possible difference in BCG properties in groups or clusters at different cosmic epochs; we return to this issue in §5.4.

### 3.2.1. Constraints from Luminosity Function Variations

First we recall the conclusion drawn from Figs 3 & 4: BCGs grow in luminosity, but at a less rapid rate compared to their host clusters. Within the hierarchical structure formation paradigm, clusters grow in mass and light by merging with other galaxy systems, and by accreting isolated field galaxies. How can BCGs grow? We examine two possibilities: (1) mergers with normal galaxies in the clusters, which, according to the calculations mentioned above, may provide a small amount of light for the BCG growth. (2) mergers with luminous galaxies, which may likely be ex-BCGs of the progenitors of the clusters under consideration. We discuss these options in turn.

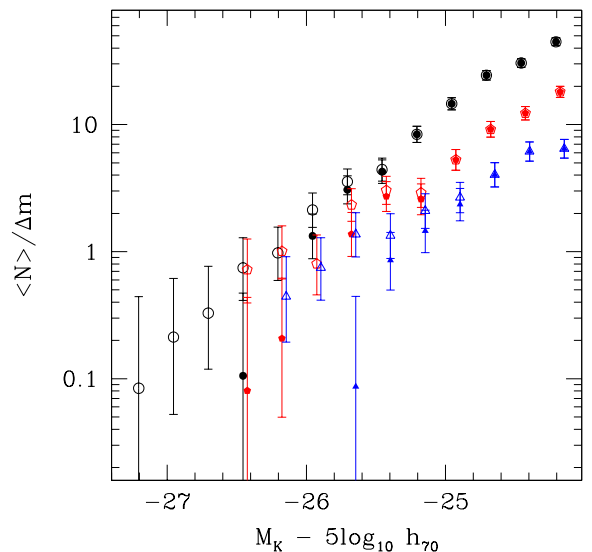


FIG. 5.— Galaxy luminosity distribution (LD: the mean number of galaxies per cluster per magnitude, with binwidth  $\Delta m = 0.25$  mag) in our cluster sample. The circular, pentagonal, and triangular symbols represent average galaxy LDs from the most massive, the intermediate, and the least massive 25 clusters. The solid symbols represent the galaxy counts when BCGs are excluded, while hollow symbols shows the whole galaxy sample. Note that the most luminous galaxies are found only in the highest mass clusters. The comparison indicates that high mass cluster LD cannot be built from LDs of intermediate and low mass clusters without galaxy mergers.

In paper II (§5.1) we study the difference between the LFs of high and low mass clusters by stacking the 25 most and least massive clusters (the mean masses are  $M_{200,h} = 7.3 \times 10^{14} M_\odot$  and  $M_{200,l} = 1.1 \times 10^{14} M_\odot$ , respectively). Two interesting points are found from the comparison: (1) the brightest galaxies appear only in the most massive clusters, and (2) there is a marked deficit of  $\sim L_*$  galaxies in high mass clusters, compared to the low mass cluster LF. We note, however, these observations refer to non-BCG galaxies, because no BCGs are included when

we construct the LFs. It is straightforward to calculate the amount of light contained in the  $\sim L_*$  galaxies that are “missing” in the high mass clusters. We integrate the difference of the low and high mass cluster LFs to obtain the luminosity density of the missing galaxy population, multiply it by the volume of a typical low mass cluster, then by the mass ratio between high and low mass systems  $M_h/M_l$ . The amount of light is  $\sim 2 \times 10^{11} L_\odot \approx 2L_*$ , about 40% of the difference between BCG luminosities in high and low mass systems ( $\sim 5L_*$ ). Therefore even if all the  $\sim L_*$  galaxies that are missing in high mass clusters were devoured by the BCG, there is still need for an additional source to feed the central beast.

To explore the second possibility, we turn to the luminosity distribution (LD) in clusters of different mass scales. The LD is the mean number of galaxies per cluster per magnitude as a function of magnitude (e.g. Schechter 1976); the difference between this and the luminosity function is that the LF contains information on spatial density of the galaxy populations. Following similar procedures outlined in §3.2 in paper II, we construct LDs for 3 mass scales; in addition to the 25 most and least massive clusters, an intermediate mass class of clusters (the mean mass being  $M_{200,i} = 2.8 \times 10^{14} M_\odot$ ) is also considered. We show in Fig 5 the resultant LDs. In the figure different point styles correspond to different mass classes. For the LD of each mass class we use two symbols to differentiate when the BCGs are included (hollow points) or excluded (solid points). It is apparent that the luminosity of the brightest galaxies in each mass class increases with the mass of the clusters. Another interesting point is that in the intermediate or high mass clusters, even non-BCG galaxies can be as bright as (or even brighter than) the BCGs in the low mass clusters (e.g. solid circles/pentagons v.s. hollow triangles). Finally, we note that there is on average  $1.0^{+0.3}_{-0.2}$  galaxy more luminous than  $M_K = -25.3$  in a typical low mass cluster, while there are on average  $3.1^{+0.5}_{-0.3}$  and  $2.0^{+0.4}_{-0.3}$  such galaxies in high and intermediate mass clusters, respectively. However, if a typical high mass cluster is composed solely from either typical intermediate or low mass clusters (i.e. no significant amount of luminous field/isolated galaxies accreted, or no significant galaxy destruction during cluster merging), we would expect there to be 5 or 6 galaxies brighter than  $M_K = -25.3$ , instead of 3, in the high mass clusters. Thus, galaxies appear to be missing on the bright end in massive clusters.

We can repeat the exercise for the amount of light expected. The observed luminosity from galaxies brighter than  $M_K = -25.3$  in a high mass cluster is  $2.2 \times 10^{12} L_\odot$ , which is at most 2/3 of the expectation if the light were coming from all galaxies in the same luminosity range in intermediate or low mass clusters. Therefore, from both galaxy counting and the luminosity budget, we conclude that there are more than enough bright galaxies in lower mass systems to make up BCGs in the most massive clusters. However, the massive cluster luminosity distributions are not simply the sum of many low mass luminosity distributions, because the massive clusters contain (1) fewer galaxies than would be expected in this case and (2) more luminous galaxies than any in the low mass clusters.

### 3.2.2. Merger Tree Considerations

The data seem to support a scenario where, after forming in low mass groups, BCGs continue to grow primarily by merging with BCGs and  $\sim L_*$  galaxies in other galaxy systems, as the host group/cluster grows hierarchically. It is important to test whether the  $\Lambda$ CDM cosmology supplies enough mergers for BCGs to grow, and if cluster light grows faster than the BCG light. We utilize a merger tree algorithm developed by Somerville & Kolatt (1999) to examine these issues. For a halo of mass  $M_0$  at  $z = 0$ , we follow the accretion/merger history of its most massive progenitor (MMP); more specifically, at each redshift step ( $\Delta z \approx 0.05$ ), we record the number and mass of haloes which merge with the MMP, the main “trunk” of the tree. For a progenitor halo of mass  $M_h$ , we estimate its galaxy content by using the halo occupation number  $N(M_h)$  determined directly from our cluster sample (paper II, §4.2). For simplicity we ignore the difference between the definition of the halo mass (i.e. that suitable for theoretical mass functions and that used as the virial masses in our observations). We also ignore any time evolution in the halo occupation number here (however, see §4.1 below).

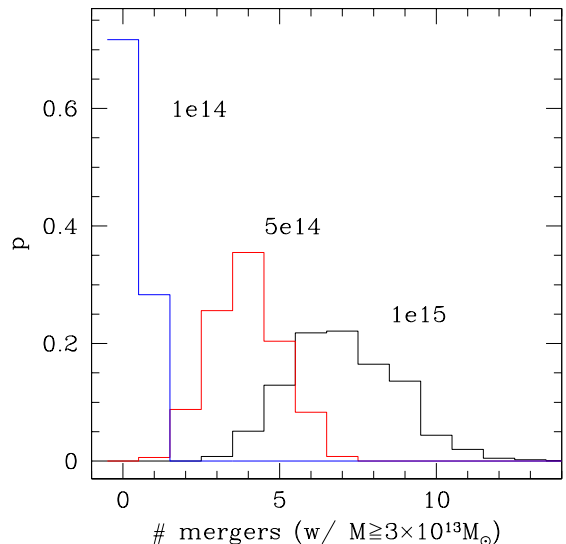


FIG. 6.— Probability distribution of the expected number of major mergers for present day clusters of different masses. The results for each halo mass ( $10^{14}$ ,  $5 \times 10^{14}$  &  $10^{15} M_\odot$ ) are generated from 1000 monte carlo realizations of merger processes, following the extended Press-Schechter formalism outlined in Somerville & Kolatt (1999). These distributions provide an indication of how many BCGs are delivered from lower mass scale groups and clusters in the formation of systems with these three masses.

We first consider the BCG growth. We estimate the numbers of massive groups ( $M_h \geq 3 \times 10^{13} M_\odot$ ) that are expected to merge onto the MMP of a present day  $M_0 = 10^{14} M_\odot$ ,  $M_0 = 5 \times 10^{14} M_\odot$  &  $M_0 = 10^{15} M_\odot$  system. With the power spectrum normalization  $\sigma_8$  adopted from the the *WMAP* result (Bennett et al. 2003) we find the numbers to be  $0.3^{+0.5}_{-0.3}$ ,  $3.9 \pm 1.1$  &  $7.2 \pm 1.8$ , respectively (Fig 6). Assuming there is at least one galaxy as bright as the observed BCGs in our lowest mass clusters ( $3 - 4L_*$ ) for each of the groups merged, and that these galaxies do not get disrupted during infall, there appears to be more than enough light to account for the luminosity differences between BCGs in each of the mass classes (c.f.



Fig 3). Furthermore, if the merger efficiency between the brightest galaxies is such that one ex-BCG from every 2–3 merged groups merges with the BCG of the main halo, the observed difference in the number of bright galaxies can be accounted for.

Next let us consider the number of (normal) galaxies to be accreted/merged with the MMP. We assume that a halo whose mass is in the range  $10^{11} \leq M_h \lesssim 10^{13} M_\odot$  contains only one galaxy, while more massive haloes follow the observed  $N(M_h)$  relation. We note that the observed  $N(M_h)$  relation is derived for galaxies brighter than  $M_K = -21$ ; from the observed galaxy luminosity function (Kochanek et al. 2001) and the theoretical halo mass function (Sheth & Tormen 1999) we estimate the mass of such galaxies to be  $\sim 10^{11} M_\odot$ . For  $M_0 = 10^{14} M_\odot$ ,  $5 \times 10^{14} M_\odot$ , &  $10^{15} M_\odot$ , we find that there are  $57 \pm 4$ ,  $205 \pm 11$  &  $373 \pm 16$  galaxies to be accreted, respectively (among these are  $36 \pm 6$ ,  $51 \pm 5$  &  $54 \pm 5$  isolated galaxies). We expect these galaxies to lose mass as they enter denser environments. Although it is possible to estimate the mass loss given a model for halo structure (e.g. Klypin et al. 1999, see §5.1 in paper II), it is not clear how the light in the galaxies will be affected. Under the assumption that the majority of these galaxies are not destroyed by tidal forces, we expect that clusters grow in their galaxy content by mainly merging with other groups/clusters, and the number of these galaxies outnumbers the ex-BCGs. We show in paper II (§4.2) that for non-BCG galaxies in clusters, light from galaxies roughly traces galaxy number (see also Rines et al. 2004). It thus appears that the increase in galaxy number due to merging with other clusters, groups and galaxies infalling from the field can account for the decreasing BCG light fraction.

It remains to be seen if the merger processes are short enough that the brightest galaxies can actually merge. This process is considered by Tremaine (1990). Consider a merger between two clusters, where both have a giant galaxy at the center. It is possible that the two giants will end up orbiting each other, and eventually merge in a time scale of about 1/5 of the Hubble time (Tremaine 1990). The “dumbbell” galaxies observed in some clusters, usually composed of two D or cD galaxies, may be in the process of merging (e.g. Quintana et al. 1996). Although the merger time scale may be short enough, definitive statements require more sophisticated numerical experiments.

### 3.3. Second and Third Ranked Galaxies

If clusters form hierarchically, the galaxies on the bright end of the LF may be themselves BCGs in progenitors that merge to form the current cluster. In the picture outlined in the previous section where the BCGs most likely grow in luminosity by merging with other bright galaxies, we can examine properties (e.g. luminosity, kinematics, etc) of the second or third ranked galaxies (G2 & G3), in hopes that they may provide some constraints on the scenario.

Using redshift information from the NED, we have secure membership assignments for 78 clusters down to G3 (82 clusters have confirmed G2). We treat these galaxies the same way as we do the BCGs (photometry,  $k$ -correction, etc). The luminosity ( $L_{G2}$ ,  $L_{G3}$ ) and the luminosity fraction ( $L_{G2}/L_{200}$ ,  $L_{G3}/L_{200}$ ) are shown in Fig 7. We see that these galaxies show trends similar

to the BCGs: the luminosity for both G2 and G3, although increasing mildly with cluster mass, becomes less important compared to total light in all galaxies in more massive systems. It is interesting to see that on average the G2s in massive clusters ( $M_{200} \geq 5 \times 10^{14} M_\odot$ ) are about as luminous as the BCGs in lower mass clusters ( $M_{200} < 10^{14} M_\odot$ ). In the lowest mass groups in our sample, the sum of the luminosities from the brightest three galaxies accounts for nearly the total light, while their sum is about 10% of total light in the most massive clusters. The similar correlations between the galaxy luminosity and the cluster bulk properties (mass and luminosity) suggest these brightest galaxies may share a similar formation history.

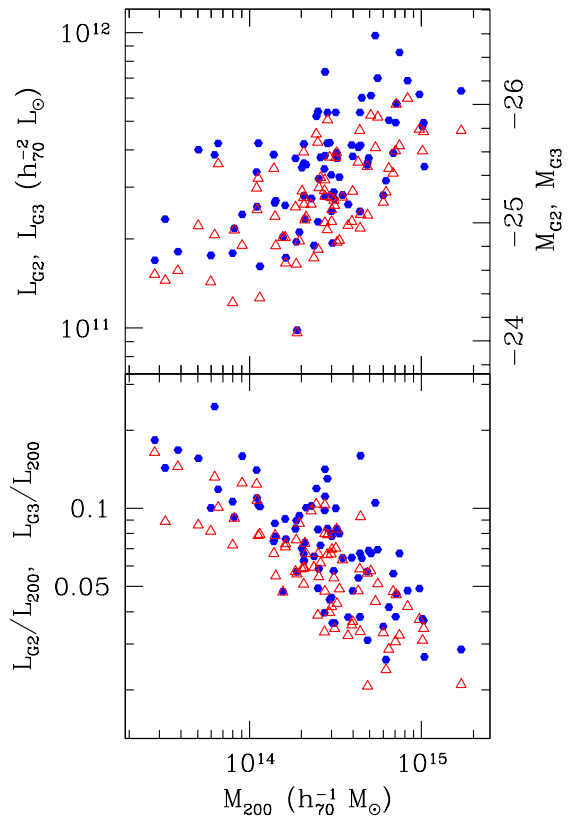


FIG. 7.— Correlations between the luminosity of the second (G2, solid points) and the third (G3, hollow triangles) ranked galaxies and cluster properties. Upper panel: Both G2 & G3 become more luminous as cluster mass increases. Lower panel: G2 & G3 luminosity-to-total luminosity fraction. On average the second ranked galaxies are 0.24 mag brighter than the third ranked galaxies (based on 78 clusters where information is available) and 0.66 mag fainter than the BCGs.

The average magnitude difference between the BCGs and G2s is 0.66 mag, with a dispersion of 0.48 mag; the same quantities for the BCGs and the G3s are 0.89 mag & 0.45 mag, respectively. The average magnitude difference between G2 and G3 is 0.24 mag, with a dispersion of 0.22 mag. We also note there is no trend between the luminosity difference and the cluster mass. Our results can be compared to that of Schneider et al. (1983b); the difference between the mean absolute magnitudes of BCGs and G2s is 0.83 mag (in  $r$  band), and that between the BCGs and G3s is 1.32 mag. Notice that their photometry

is measured within a fixed metric radius of  $13.7h_{70}^{-1}$  kpc.

We also examine the projected distribution of the G2s with respect to the BCGs, as a function of cluster mass. We find no apparent evidence that suggests the G2s in more massive clusters lie closer to the BCGs. As for the velocity differences between the two brightest galaxies, a Kolmogorov-Smirnov test indicates a weak possibility that the velocity differences (scaled by the cluster mean velocity dispersion) in clusters more massive than  $M_{200} = 2.8 \times 10^{14} M_{\odot}$  is different from those found in lower mass clusters (a 9% chance that the two distributions are the same). These findings do not provide strong indications of a kinematic relationship between the BCGs and G2s; we suggest that a larger cluster sample with a targeted spectroscopic study would be an interesting way to further probe for a relationship.

#### 4. CONSTRAINTS ON INTRACLUSTER LIGHT

It has long been suggested that dynamical processes will alter or transform properties of galaxies that orbit in clusters (e.g. Gunn & Gott 1972; Merritt 1984; Moore et al. 1998; Treu et al. 2003, and references therein). Mergers, galaxy harassment, tidal truncation, and ram pressure stripping may all liberate galactic material (dark matter, stars, gas, etc) into the intergalactic space (e.g. Malumuth & Richstone 1984; Gnedin 2003; Napolitano et al. 2003; Sommer-Larsen et al. 2004; Murante et al. 2004; Willman et al. 2004). Observations have provided ample evidence to support this inference. Intracluster stellar populations are detected in various forms, as reviewed in §1 (see also Arnaboldi 2003; Feldmeier et al. 2003c for more complete account). These may well be the source of the ICL, as well as the diffuse haloes/envelopes of the cD galaxies. We emphasize here that no distinction between ICL and cD envelope is made in this paper.

There must be another component in clusters that accounts for the light lost from the galaxies. This component is bound to the cluster, but may or may not be distributed like the galaxies. We identify this component as the ICL. In general, we expect ICL to become more and more important in the overall light budget in massive clusters. However, the detailed behavior would of course depend on the complicated dynamical history of clusters, as well as the galaxy formation efficiency across the mass spectrum of clusters. In §4.1 we propose simple models to estimate the ICL light fraction as a function of cluster mass, and compare these predictions with available observational constraints.

In addition to confirming this dynamical view of galaxy-cluster interactions, studies of the ICL may provide a more accurate determination of the cluster baryon fraction and cold fraction (defined as the ratio between stellar mass and total baryon mass in clusters), which in turn should help clarify the star formation efficiency in clusters (§4.2). Finally, the ICL may serve as an important source of the enrichment of the intracluster medium (ICM). The ICM is known for its high metal abundance ( $\sim 0.3Z_{\odot}$  for iron, De Grandi et al. 2004 and references therein). Apparently the metal comes from stars, i.e. via supernova explosions. The large amount of metal present in the ICM can not be accounted for with standard chemical yields or metal transport mechanisms such as galactic winds (e.g. Porti-

nari et al. 2004); confined by the potential wells of individual galaxies, the efficiency of the enrichment processes is not high. On the contrary, supernovae orbiting in the intracluster space surrounded by the ICM or supernovae in low mass, pregalactic structures, may be much more efficient agents of enrichment. In §4.3 we use the predicted amount of ICL to reevaluate the enrichment problem in the ICM (see also Zaritsky et al. 2004).

##### 4.1. Estimating the Intracluster Light

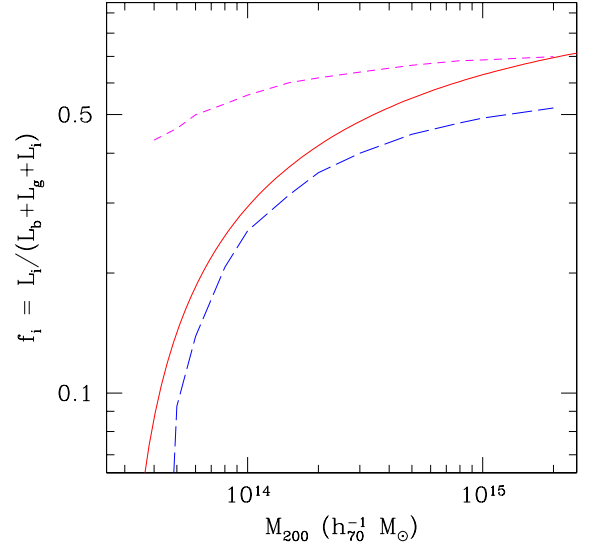


FIG. 8.— Estimated ICL fraction. The solid curve corresponds to the prediction of Eqn 2, with  $\sim 1\%$  of light in ICL in lowest mass groups ( $M = 3 \times 10^{13} M_{\odot}$ ). The two dashed lines are the predictions from a merger tree model (Eqn 3), with two models for redshift evolution of the light-mass relation (long-dashed: no-evolution,  $\gamma = 0$ ; short-dashed:  $\gamma = 1$ , evolution consistent with numerical simulations).

We decompose the total light in a cluster into three components:

$$L_{tot} = L_b + L_g + L_i,$$

where the terms on the right hand side denote the light of the BCG, the other galaxies, and the ICL, respectively. In general, we expect all these components to be functions of cluster mass. Next suppose there is a system (of mass  $M_{\ell}$ ) that serves as a building block of systems more massive than  $M_{\ell}$ . We denote

$$L_{tot,\ell} = L_{b,\ell} + L_{g,\ell} + L_{i,\ell}$$

for this system. If clusters grow in mass and luminosity mainly by mergers between such systems (i.e. accretion of field galaxy populations is not important), then we can write  $L_{tot}(M) = (M/M_{\ell})L_{tot,\ell}$ ; in this case the ICL light for a system of mass  $M$  is simply

$$L_i(M) = \left(\frac{M}{M_{\ell}}\right) L_{tot,\ell} - L_b(M) - L_g(M). \quad (2)$$

If we set the mass scale  $M_{\ell}$  to be that of the least massive group in our sample ( $\sim 3 \times 10^{13} M_{\odot}$ ), using our observed behavior for  $L_b(M)$  and  $L_g(M)$ , we would then be able to predict the amount of ICL as a function of cluster mass, with the value for ICL in groups of mass  $M_{\ell}$ ,  $L_{i,\ell}$ , being a free parameter. This approach is effectively saying that

TABLE 2  
 SOME OBSERVATIONAL CONSTRAINTS ON THE ICL FRACTION

Name	Virial Mass ( $10^{14} M_{\odot}$ )	Band /Method	Depth (mag/arcsec <sup>2</sup> )	Extent	$f_{i,2D}$	Reference
A2390	14.9	r	26.7	204 kpc ( $0.09 r_{200}$ )	$0.02 \pm 0.06^{\dagger}$	1
A2029	11.2	R	26.0	360 – 640 kpc ( $0.18 - 0.32 r_{200}$ )	0.1	2
A1656	9.7	R	27.7	8' ( $0.12 r_{200}$ )	0.5	3
A1689	9.6	R	28.2	143 kpc ( $0.07 r_{200}$ )	0.3	4
A1914	9.4	V	26.0	1.6 Mpc ( $0.84 r_{200}$ )	0.28	5
A1413	6.4	V	26.5	180 kpc ( $0.10 r_{200}$ )	0.13	6
A1651	6.2	I	29.5	714 kpc ( $0.42 r_{200}$ )	$0.38^{\ddagger}$	7
Cl0024+1652	3.4	V	N/A	153 kpc ( $0.12 r_{200}$ )	$0.15 \pm 0.03$	8
A2670	2.7	R	29.0	3.5' ( $0.23 r_{200}$ )	0.3	9
Virgo	1.5	ICPNe <sup>‡</sup>	27.4	0.196 deg <sup>2</sup>	$0.10^{\dagger}$	10,11
		ICPNe <sup>‡</sup>	27.0	0.89 deg <sup>2</sup>	$0.16 \pm 0.03^{\dagger}$	12
		I/ICRGB <sup>§</sup>	27.9	4.73 arcmin <sup>2</sup>	$0.1 - 0.2^{\dagger}$	11
HCG90	0.19	V	24.5	64 arcmin <sup>2</sup>	$0.45 \pm 0.05$	12
M81 group	$0.012^b$	ICPNe <sup>‡</sup>	N/A	1.44 deg <sup>2</sup>	$0.013^{\dagger}$	13
Leo I group	N/A	ICPNe <sup>‡</sup>	24.7	0.26 deg <sup>2</sup>	$< 0.016^{\dagger}$	14

Note. —  $h_{70} = 1$  is assumed in calculating the mass  $M_{200}$  and size. References: (1) Vilchez-Gomez et al. (1994); (2) Uson et al. (1991); (3) Bernstein et al. (1995); (4) Tyson & Fischer (1995); (5) Feldmeier et al. (2004b); (6) Feldmeier et al. (2002); (7) Gonzalez et al. (2000); (8) Tyson et al. (1998); (9) Scheick & Kuhn (1994); (10) Okamura et al. (2002) (11) Arnaboldi et al. (2003) (12) Feldmeier et al. (2004a); (13) Durrell et al. (2002); (14) White et al. (2003); (15) Feldmeier et al. (2003b); (16) Castro-Rodríguez et al. (2003). <sup>†</sup>: excluding BCG envelope. <sup>‡</sup>: including BCG light. <sup>‡</sup>: derived from intracluster planetary nebula (ICPN) abundance. <sup>§</sup>: derived from intracluster RGB star (ICRGB) abundance. <sup>b</sup>: Karachentsev et al. (2002).

the lower galaxy luminosity per unit cluster mass in massive clusters (recall that the slope of the  $L$ – $M$  relation is less than unity) is simply because stars have been stripped off galaxies during the hierarchical merging that produced the high mass clusters from the low mass clusters.

In Fig 8 we show the predicted ICL light fraction  $f_i \equiv L_i/L_{tot}$  of this toy model (solid line), assuming that  $q \equiv L_{i,\ell}/(L_{b,\ell} + L_{g,\ell}) = 0.01$ , that is, an ICL that is 1% of total light in galaxies for groups of mass  $M_{\ell}$ . The predicted ICL fraction is high. For clusters more massive than  $10^{14} M_{\odot}$ ,  $f_i > 0.3$ ; at  $10^{15} M_{\odot}$ , about 2/3 of total light is in the intracluster space! This estimate does not change much if we choose different values for  $q$ ; for  $q = 0.05$  or  $q = 0.10$  the ICL fraction is similar to the curve of  $q = 0.01$  for systems more massive than  $10^{14} M_{\odot}$ .

Effectively, Eqn 2 assumes that the stellar mass fraction is constant in clusters of different mass, which may not be the case. Furthermore, the toy model neglects the accretion of isolated galaxies, which may be important (§3.2.2). We therefore consider a second model which utilizes the merger tree algorithm used in §3.2.2. The basic idea is to estimate the total light content of a cluster by counting luminosities contained in all the galactic systems that fall into the cluster, and compare it with the observed light in cluster galaxies. The difference would then be the ICL. To this end, we need a light–mass relation for galactic systems ranging from single galaxies to clusters. For systems more massive than  $10^{13} M_{\odot}$ , we employ the observed  $L$ – $M$  relation (§4.1 in paper II); for less massive systems, which we assume to be single galaxies, we estimate their  $L$ – $M$  relation by matching the number densities indicated by the observed  $K$ -band galaxy luminosity function (Kochanek et al. 2001) and that predicted by the theoretical halo mass function (modulated by the halo occupation num-

ber; Kravtsov et al. 2004).

By summing over the light of each galactic system that has merged directly onto the main trunk of the tree (the MMP), we can estimate the total light as a function of the cluster mass. To be more specific, for a present-day cluster of mass  $M_0$ , we calculate

$$L_{tot}(M_0) = \sum L_h(M_h) (1 + z_h)^{\gamma}, \quad (3)$$

where  $M_h$ ,  $L_h$  and  $z_h$  correspond to the mass, the luminosity of the merged haloes, and the epoch of the merger, respectively. The redshift dependence is included to account for any evolution in the  $L$ – $M$  relation or halo occupation number (Kravtsov et al. 2004, §5.3 in paper II). We consider two possibilities:  $\gamma = 0$  &  $\gamma = 1$ . The former is the no-evolution case, while the latter is consistent with the halo occupation number evolution as suggested by numerical simulations (Kravtsov et al. 2004).

The predictions of this second model are shown in Fig 8 (averaged over 100 merger tree realizations): The long-dashed line refers to the  $\gamma = 0$  case, while the short-dashed line shows the  $\gamma = 1$  results. Interestingly the model results for the two values of  $\gamma$  enclose the predictions of the first model. We note that the second model does not account for any ICL contained in the galactic systems that merge with the main halo; the predictions thus are lower limits on the ICL light fraction.

To compare these predictions with estimates derived from direct observations, we compile in Table 2 several published values. The columns give the name of the cluster, the virial mass estimated from published X-ray measurements, the band used, the physical or angular extent of the observation, the measured ICL fraction, and the original reference. Some remarks may help the reader. First of all, these studies use different bands, have different depth,

and survey different fractions of the clusters. We caution that the ICL fraction may depend on the waveband used (Vilchez-Gomez et al. 1994). Our estimate is given in  $K$ -band for galaxies brighter than  $M_K = -21$  mag (recall that we integrate the LF to  $M_{min} = -21$  mag, §2.1). For the nearby clusters or groups, it is possible to estimate the ICL fraction from tracers such as intracluster planetary nebulae (ICPNe) or RGB stars. However, these techniques look for patches in the cluster/group fields and we only list the total area of the observations, but not the fraction of the virial radius surveyed. Finally, strictly speaking, the ICL fraction listed in the Table is the projected value, while the prediction of our model is that contained in the 3D cluster region. To compare the values a model for the radial distribution of ICL is needed.

In addition to these observations, a recent study stacking a large number of clusters suggests the ICL contributes about 15 – 20% of cluster optical light within 500 kpc (Zibetti & White 2004). A recent measurement of BCG+ICL profile for a sample of 24 clusters is presented in Gonzalez et al. (2004).

Finally, we compare these simple models with the findings from numerical studies. The modeling by Napolitano et al. (2003) uses an  $N$ -body simulation of a Virgo-like cluster formed in a hierarchical fashion to study the distribution and correlation properties of tracers of ICL. They estimate that outside the central region, the ICL fraction may be 30 – 50%. A big step forward toward theoretical modeling of the ICL is realized in the recent cosmological hydrodynamic simulations (Murante et al. 2004; Sommer-Larsen et al. 2004; Willman et al. 2004). In particular, the former study finds that the ICL fraction increases with cluster mass, in broad agreement with our results. At  $M_{200} = 10^{14} M_\odot$  their model predicts  $f_i \approx 0.25$ , while at  $M_{200} = 7 \times 10^{14} M_\odot$  the ICL fraction is about 0.45; although it is encouraging that both these values are very close to the predictions of our second model with  $\gamma = 0$ , a comparison between our local clusters and clusters at higher redshifts suggests a nonnegligible evolution in the halo occupation number (see §5.3 of paper II). Further investigations on the halo occupation number evolution, as well as higher resolution numerical studies, are needed to resolve this discrepancy.

The two models presented here, as well as other numerical studies, suggest that the ICL can be very important in the overall cluster light budget; we discuss some of the implications next.

#### 4.2. ICL Contribution to Cluster Baryon Fraction

An immediate implication of these estimates is that the baryon fraction and cold fraction derived from galactic light need revision. Because of the relatively small contribution of stars in galaxies to the baryon budget (§4.1 in paper I), a roughly 100% increase in stellar mass would not change the baryon fraction or the derived  $\Omega_M$  constraints much. Within our sample of 93 clusters, we have measured ICM gas mass for 35 (which we denote as the MME subsample, Mohr et al. 1999). Based on these clusters, the mean baryon fraction is 0.1441, while for “hot” clusters (which we choose to have  $kT_X \geq 3.7$  keV, see §3 in paper I), the mean is 0.1512. Using the value for

baryon density from *WMAP* (Bennett et al. 2003), these correspond to  $\Omega_M = 0.32$  & 0.30, respectively. Now, from Fig 8 we can roughly estimate that the total light (including the ICL) would be  $\sim 2(L_b + L_g)$ . This assumption leads to  $\Omega_M = 0.29$  & 0.28, for the MME subsample and the hot clusters within it, respectively. Both these values are in good agreement with the *WMAP* estimate of  $\Omega_M = 0.27 \pm 0.04$ .

The presence of ICL has a more significant effect on the cold fraction; for the MME subsample and the hot clusters within it, the mean values are 0.150 & 0.163, respectively. Compared to the mean values when no ICL is present (c.f. §4.2 in paper I), these correspond to a 40% increase. Interestingly, a recent cosmological hydrodynamical simulation (Borgani et al. 2004) finds that roughly 20% of baryons are cold for clusters hotter than 3 keV (roughly  $M_{200} \sim 2 \times 10^{14} M_\odot$ ). The current implementation of feedback/heating mechanisms may not be far from producing the cold fraction in real clusters.

#### 4.3. Enrichment of Intracluster Medium

It is well established that the ICM contains an enormous amount of metal (e.g. Arnaud et al. 1992; Loewenstein & Mushotzky 1996; Finoguenov et al. 2000; De Grandi & Molendi 2001; Baumgartner et al. 2003). Within standard models for star formation in galaxies and the processes that transport metal to the intracluster space, a standard stellar initial mass function (IMF) with typical supernova yields can not account for the metal production (e.g. Portinari et al. 2004, hereafter P04). Non-standard scenarios such as a time-varying IMF, IMFs that differ in different environments, or different enrichment agents (e.g. hypernovae from population III stars) have been proposed as alternatives (e.g. Finoguenov et al. 2003; Loewenstein 2001, P04).

Here we investigate to what degree the ICL can help account for the extraordinary metal production in clusters. We will focus on the iron abundance. Following the same procedures outlined in §4.3 in paper I (with the latest ICM iron abundance from a sample of 22 clusters observed with *BeppoSAX*,  $Z_{ICM,Fe} = 0.34Z_{\odot,Fe}$ ,<sup>5</sup> De Grandi et al. 2004, hereafter DG04), we estimate the iron yield (Arnaud et al. 1992)  $y_{Fe} = (M_{Fe,ICM} + M_{Fe,star})/M_{star}$  and the iron mass fraction (the iron-to-total mass ratio) for the MME subsample. Two important quantities involved in the calculations of iron mass in stars are the mean stellar mass-to-light ratio and the metallicity. We use the observed typical stellar mass-to-light ratio and metallicity for early and late type galaxies, weighted by the relative abundance of the two types in clusters as a function of cluster mass, to account for possible variations of these quantities with respect to cluster mass (see Appendix of paper I for more details). In Fig 9 (upper panel) we show the iron yields obtained without ICL (shown as hollow points). As we find in paper I, the iron yield is very high ( $3 - 9Z_{\odot,Fe}$ ) compared to the solar vicinity ( $0.9 - 0.95Z_{\odot,Fe}$ , P04) and is an increasing function of cluster mass, while the iron mass fraction is roughly constant with respect to cluster mass.

The inclusion of the ICL reduces the iron yield. With the amount of ICL predicted by our first model (Eqn 2, c.f.

<sup>5</sup> this is the value based on the revised solar photospheric abundance (Grevesse & Sauval 1999), which implies iron mass fraction  $X_{\odot,Fe} = 0.0012$ .

Fig 8), the corresponding iron yield falls to about  $3Z_{\odot, Fe}$  (solid points in the upper panel). We note, however, in this case the iron mass fraction (total iron mass over total binding mass; not shown in this figure) becomes a weakly increasing function of cluster mass.

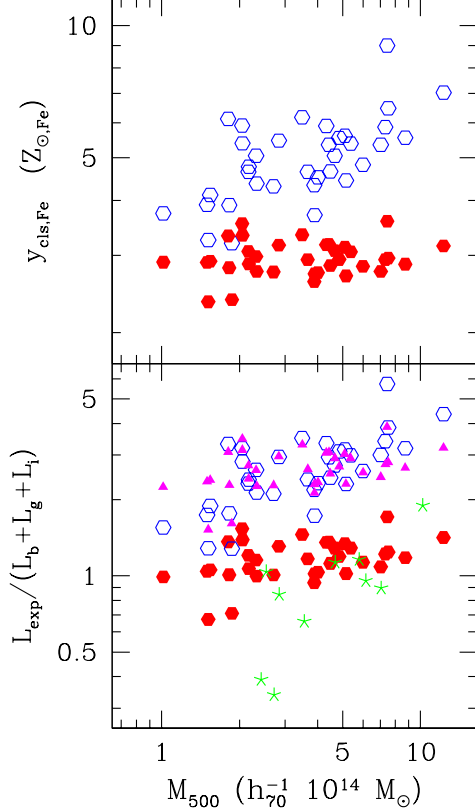


FIG. 9.— Upper panel: the iron yields in the MME subsample. The hollow points show the results derived without any ICL, while the solid symbols are the yields when an ICL given by Eqn 2 is included. The ICL reduces the yields and makes them roughly constant for clusters of all masses. Lower panel: the ratio between the total light required to produce the observed iron (in stars and ICM) and the total observed cluster light. The solid hexagons and triangles show the cases for Salpeter & Kroupa IMFs, respectively, and in these cases the ICL contribution to the total light is included. The hollow points show the Salpeter case with no ICL included. Note that in the Salpeter IMF model, there is enough stellar light (when ICL is included) to explain the enormous iron reservoir. The stellar symbols show the ratio of the luminosity required to produce the “iron excess” in cool core clusters compared to ICL+BCG luminosity. In most cases the ICL is crucial in producing the excess iron component. Note the ordinate is  $M_{500} \approx 0.72M_{200}$ , the mass enclosed by the radius  $r_{500}$  (see §2.1).

To further quantify the possible role of ICL in the ICM enrichment, we compare the predicted iron mass-to-total light (ICL and galaxies) ratio (IMLR, Renzini et al. 1993) with the single stellar population (SSP) models of P04. Specifically, given an initial mass function, a SSP model predicts the evolution of stellar mass and luminosity, as well as its iron production. One can thus compute the IMLR at any epoch. For a stellar population of 10 Gyr old, we calculate the total light required for a cluster IMLR to be consistent with the SSP prediction. We show the ratio between the required luminosity ( $L_{exp}$ ) and our observed luminosity ( $L_{tot} \equiv L_b + L_g + L_i$ ) for each cluster in Fig 9 (upper panel), with ICL given by Eqn 2. The solid

hexagons and triangles show the cases for the Salpeter (1955) and the Kroupa (2002) IMF, respectively. We note that the latter IMF describes the solar neighborhood better than the former (P04). For comparison, we also show the case for the Salpeter IMF when no ICL is included (hollow symbols).

From this figure we draw the following conclusions: (1) for the Salpeter case, the observed light plus the ICL is slightly lower than that required to produce the observed iron (the mean is  $\overline{L_{exp}/L_{tot}} = 1.17 \pm 0.04$ ; no theoretical uncertainty is included), but there is a severe shortage of stars and luminosity when a Kroupa IMF is used to produce the observed iron (the mean is  $2.66 \pm 0.08$ ); (2) when no ICL is present, even with the Salpeter IMF, the required total light is about 2.7 times the observed light from all galaxies, and with the Kroupa IMF, the situation worsens to a factor of 6 more light required; (3) the iron production efficiency becomes more uniform across different mass scales when the ICL is included, as can be inferred from the shallow slope ( $0.14 \pm 0.05$  for both IMFs) of the  $L_{exp}/L_{tot}$ -mass correlations, as well as the iron yields. Without the ICL, the steep slope of the  $L_{exp}/L_{tot}$ -mass correlation ( $0.38 \pm 0.07$ , hollow points) shows an increasing need for an extra light component (or more efficient iron production) in more massive clusters.

ICL may also help with the “iron excess” found in clusters with cool cores. The radial distribution of the iron abundance is distinctly separated into two forms: (a) a nearly flat distribution for the clusters without a cool core (NCC—non-cool core clusters), and (b) a centrally peaked profile for the cool core (CC) clusters. The amount of iron from the central part of CC clusters above the uniformly distributed iron floor (seen also in NCC clusters) is called the iron excess. Using a sample of 12 CC clusters, DG04 examine the relation between the BCGs and the iron excess in the clusters. Using standard stellar population synthesis models, they find the extra amount of iron is comparable to the iron in supernova ejecta from the BCGs.

Here we evaluate the role of ICL (and BCG) in this process in a very simple way; given the excess iron mass in a cluster, we calculate the expected amount of light in the core, if the IMLR for the excess iron is to be consistent with a SSP model. We have the BCG luminosity for 10 of 12 CC clusters in the DG04 sample (excluding A2142), and we again use Eqn 2 to estimate the amount of ICL within the central  $0.2r_{200}$  of the clusters (assuming the ICL is distributed similarly to the galaxies, namely an Navarro et al. 1997 profile with concentration of 3, see §3.1 in paper II). We use the value of the iron excess provided in Table 1 of DG04. The ratio between the SSP IMLR-inferred total light (Salpeter IMF) and our ICL+BCG light is shown as stars in the lower panel of Fig 9. It is clear that for some clusters, the BCG alone may account for the iron excess, but in other cases ICL helps to provide sufficient iron. Repeating the calculations for the Kroupa IMF, we find that on average  $\overline{L_{exp}/(L_b + L_i)} = 2.1 \pm 0.3$ . Assuming a more concentrated radial profile for the ICL (e.g. the de Vaucouleurs profile found by Gonzalez et al. 2004), we find that  $0.2 \leq \overline{L_{exp}/(L_b + L_i)} \leq 0.9$  for the Salpeter IMF. It is clear that the ICL reservoir of stars is helpful in explaining the iron excess in cool core clusters.



To summarize, we find that: (1) the ICL lowers the mean iron yield per solar mass of stars for the cluster iron production, although the value is still high compared to that of the solar vicinity; (2) it is possible to generate the amount of iron observed in clusters with the yields consistent with simple stellar population models, if a Salpeter IMF is assumed and an ICL amount predicted by our model is present; (3) the ICL makes the production efficiency of iron more uniform for clusters of different masses, which is reflected in the near-flat iron yields and the flat  $L_{exp}/L_{tot}$  ratios, with respect to cluster mass; (4) the ICL can help in the production of the excess iron in the cores of CC clusters (by lowering the yields and shortening the enrichment time, c.f. Böhringer et al. 2004). The ICL not only helps produce the metals, but also circumvents the problem of transporting the metals out of galaxy halos and into the ICM. However, if the IMF is consistent with that observed in the solar vicinity, simple stellar population models require more than twice as much more light to explain the iron production in clusters.

We note that the above calculations only deal with the *amount* of iron that can be produced, but not the relative abundances between iron and other elements. More sophisticated models that also invoke an ICL component are needed to fully investigate the ICM enrichment process.

## 5. DISCUSSION

### 5.1. Choice of Photometry

As a test of the robustness of our results, we conduct the analysis presented in §3.1 using the 2MASS extrapolated total magnitudes for the BCGs. We find that it makes no difference on the  $L_b$ - $M$  relation whether isophotal (corrected by 0.2 mag) or total magnitudes are used.

In this paper we choose not to examine the BCG light from magnitudes measured at a fixed metric radius, as many investigators do (e.g. Schneider et al. 1983b; Brough et al. 2002). The reason is that the sizes of BCGs are not fixed; we find that the half-light radius of the BCGs correlates with mass of the host cluster. Using the isophotal magnitudes has the advantage of reflecting this correlation, which may provide some insights into the BCG formation histories.

### 5.2. BCG Sample Selection

Our cluster sample is basically X-ray selected, which may bias against those loose, low mass systems whose X-ray emission is weak. In order to assess the effects of this possible bias on the BCG properties, we investigate the properties of the BCGs in a large sample of optically selected groups and clusters (the UZC-SSRS2 group catalog, hereafter UZC groups, Ramella et al. 2002). For each member galaxy we search in the 2MASS extended source catalog its  $K$ -band counterpart within  $25''$  of the position listed in the catalog. We focus on groups of five or more members that are distinct from our sample clusters and groups. Note that only 40 – 80% of the UZC groups with five or more members are estimated to be real physical systems (Ramella et al. 2002). The virial mass for each group is from Table 1 of the catalog (Ramella et al. 2002).

In Fig 10 we compare the properties of these BCGs with those in our sample. The upper panel shows the  $L_b$ - $M$  correlation (the crosses are 291 UZC groups, the squares are

the UZC groups that have detected X-ray emission from the *ROSAT* All-Sky Survey, Mahdavi et al. 2000, and the shaded area show the distribution of BCGs in our sample). We see that the X-ray-bright UZC groups seem to occupy the same regions in the  $L_b$ - $M$  space, if only somewhat less massive, while the X-ray-faint groups exhibit large scatter in both BCG luminosity and system mass. Possible sources for the scatter include: (1) 20 – 60% of these systems may be chance projections (i.e. not real); (2) uncertainties in the estimated virial mass; 65% of the systems have only five members; we note that with only 5 (10) redshift measurements, the fractional  $1\sigma$  uncertainty in mass is about 95% (67%). Even in the limit that a large number of redshifts is available, the dynamically inferred mass may still be affected by the presence of substructure or surrounding large scale structure. A comparison between X-ray-derived mass ( $M_X$ ) and velocity dispersion-inferred mass ( $M_V$ ) for 8 massive ( $M_{X,200} \geq 5 \times 10^{14} M_\odot$ ) clusters in common between our sample and the UZC catalog shows that the average mass difference is  $\bar{M}_V/M_X = 6.5$  (number of redshifts based on which dynamical masses are derived ranges from 19 to 144; the smallest and largest  $M_V/M_X$  ratios are 1.9 & 12.3, which are from 144 & 72 redshifts, respectively). Although there is a correlation between the number of redshifts measured and the mass difference, some outliers that strongly deviate from the correlation exist. In our analysis we regard the X-ray emission weighted temperature as a more reliable mass estimator.

Under the assumption that the clusters are largely regular systems, at a given mass we expect a cluster to contain a certain number of galaxies (e.g. from the observed  $N$ - $M$  relation). We therefore can select only groups whose number of members is at least 10% of the expected galaxy number based on our observed  $N(M)$  relation; with this requirement, for a given BCG luminosity, clusters in our sample represent the most massive systems (i.e. crosses that lie on the lower right part of the shaded area will be removed by this criterion).

Comparing the BCGs in the X-ray-bright UZC systems (squares) with those in our sample (shaded region), we see that there is no suggestion of flattening of the  $L_b$ - $M$  correlation below  $10^{14} M_\odot$  (c.f. §3.1). For a given cluster mass, this comparison shows how much scatter there may be for the luminosity of BCGs in the local universe.

The lower panel of Fig 10 shows the BCG light fraction for a subset of the UZC groups (crosses). We only show those systems which lie close enough so that the 2MASS probes down to or below  $M_K = -21$ . These systems seem to form a continuation from our sample (solid points) in their BCG light fraction. This is interesting, because the two samples are selected very differently (optical vs X-ray); however, we caution again that mass uncertainties in the low mass UZC groups may be large. The crosses surrounded by a square show the groups with ten or more redshift measurements. The BCG light fraction in these groups is indeed consistent with the expectations from our sample. We infer that the galaxy formation process is highly regular, and that the halo mass is the single most critical parameter in determining the BCG light fraction.

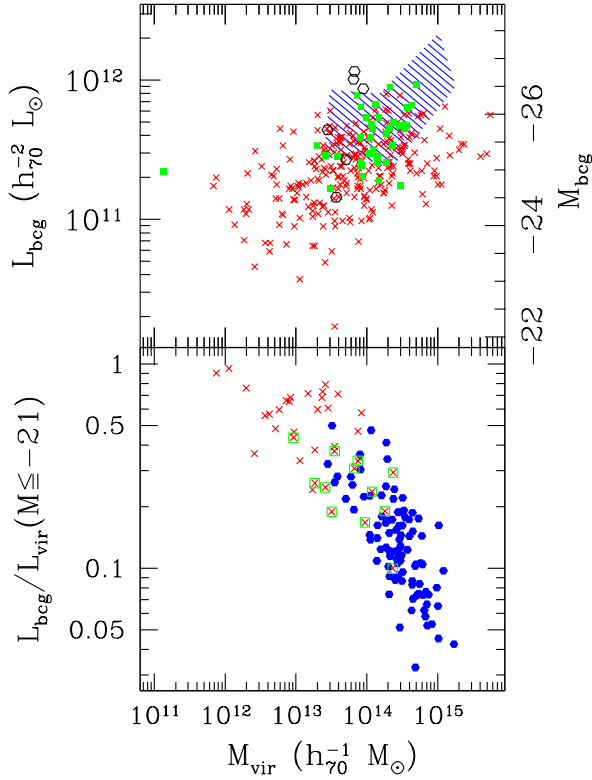


FIG. 10.— Upper panel: the BCG luminosity for the UZC systems (the crosses) and for our sample (shaded area); those UZC systems with detected X-ray emission are denoted by squares. (Circles: the “fossil group” BCGs, see §5.3.) Lower panel: the BCG contributions to the total light emitted from galaxies. The crosses are the UZC BCGs, the crosses with a square are the UZC groups with ten or more redshift measurements, the solid points are BCGs in our sample. We only show the UZC systems that are probed down to at least  $M_K = -21$  by the 2MASS.

### 5.3. Fossil Groups

There exists a class of galactic systems with masses comparable to groups of galaxies, with diffuse X-ray emission from hot gas, but where the optical light is totally dominated by one single galaxy (the so-called “fossil groups”, e.g. Jones et al. 2003 and references therein). One property for a group to qualify as a fossil group is that the (optical) magnitude difference between the brightest and second ranked galaxies exceeds  $\Delta m_{12} \geq 2$ . This in turn implies that the BCG luminosity fraction in these groups is large (e.g. 70%, Jones et al. 2003, hereafter J03). Based on an X-ray flux-limited sample, J03 suggest that the fossil groups constitute 8 – 20% of all systems with comparable X-ray luminosity ( $L_X \geq 5 \times 10^{41} h_{70}^{-2}$  erg/sec), and may be an important source for producing the BCGs in more massive systems (after the groups fall into larger systems). We show in Fig 4 that in the lowest mass systems in our sample, the BCG light fraction approaches 50%. Our merger picture of BCG growth also implies that the BCGs in lower mass systems serve as building blocks for the brightest galaxies in more massive systems.

To examine whether these fossil groups are different

from our low mass groups, we identify the six fossil group dominant galaxies listed in Jones et al. (2000, 2003) in the 2MASS extended source catalog, and estimate the group mass from either X-ray luminosity or temperature. The masses of these systems are estimated to lie in the range  $2 - 9 \times 10^{13} M_\odot$  (again, we caution large uncertainties in mass). Compared to our BCGs and those in the UZC groups, half of the fossil group galaxies show extraordinary luminosity in the sense that they are 0.3 – 0.5 mag brighter than expected for the mass of their host groups (Fig 10, upper panel, hollow circles). The other half appear at normal or even dimmer luminosity within the mass range (we note, however, that no lower limit on the BCG optical luminosity is imposed in J03’s criteria for fossil groups). Due to the depth of 2MASS, it is not possible to further examine the luminosity fraction of these galaxies in  $K$ -band. However, there is one system in each of our sample and the UZC catalog that appears to be a fossil group: AWM04 & U085. Both have  $\Delta m_{12} > 2$  in  $K$  and are X-ray luminous. The BCG luminosities are  $7.1 \times 10^{11} h_{70}^{-2} L_\odot$  &  $7.8 \times 10^{11} h_{70}^{-2} L_\odot$ , and the BCG light fractions are 0.41 &  $< 0.63$ ,<sup>6</sup> respectively. The BCGs of these two systems are slightly more luminous than the expectation from Eqn 1, and the BCG luminosity fractions do not show a total dominance. Based on only few systems, it is not possible to draw definitive conclusions. However, it is suggestive that the fossil groups found in J03 are a natural extension in the very low mass regime of the BCG behavior found for the large cluster sample studied in this paper. Larger cluster samples and deeper photometry will be needed to better examine this possibility.

### 5.4. BCG Formation Scenarios

In §3.2 we discuss some possible BCG evolution scenarios. Currently both observational and numerical studies favor the theory that BCGs form rapidly from mergers of several galaxies during an early epoch of cluster or group collapse, followed by a rather limited subsequent growth in luminosity (e.g. Merritt 1984; Lauer 1988; Tremaine 1990; Dubinski 1998; Oegerle & Hill 2001). We argue, however, that BCGs have to merge with other galaxies, most likely the BCGs from merging groups, as they are the most efficient source of light for the BCG light growth. Support for this picture includes the fact that (1) moderately luminous ( $\sim L_*$ ) galaxies that are more abundant in low mass clusters do not contain enough light to account for the growth in BCG luminosity, (2) there are enough very luminous galaxies available to account for the BCG luminosity growth, (3) massive galaxies can indeed merge within relatively short timescales (Tremaine 1990) and (4) massive galaxies are more likely to merge because of the larger cross sections (or gravitational focusing) and shorter dynamical friction timescales (e.g. Klypin et al. 1999).

In such a scenario, the BCG co-evolves with the cluster. The tight correlation between the BCG light fraction and cluster mass strongly supports this view. The scatter in the BCG light on group scales may reflect the heterogeneous origin of these galaxies (c.f. Figs 3, 10); if they were the outcome of mergers among several massive galaxies during cluster collapse, we do not expect their proper-

<sup>6</sup> Note that the total light in U085 is estimated to  $M_K = -22.1$  only. We have ignored the criterium that  $\Delta m_{12} \geq 2$  is to be applied for galaxies within half of the virial radius (J03).

ties to be as homogeneous as those in high mass clusters. However, as these building blocks merge and form more massive BCGs, the mixing makes their properties more homogeneous.

One possible consequence of the merger is that BCGs in more massive clusters may have different structure than those in low mass systems. We find that the half-light radius  $r_e$  of the BCGs positively correlates with cluster mass. Deep photometry, which is needed for examination of other structural parameters, such as  $\alpha \equiv d \log L / d \log r|_{r_m}$ , the logarithmic luminosity derivative at a fixed metric radius  $r_m$  (e.g. Hoessel 1980; Postman & Lauer 1995, however, see Collins et al. 2003), or spectroscopic studies that reveal the stellar kinematics of the BCGs to large radii (e.g. Weil & Hernquist 1996), may further test this evolution scenario. Although we expect these mergers to be mainly without star formation, color information may provide valuable clues.

Our suggestion for BCG light (mass) growth comes from the clusters in the nearby universe; by studying the BCGs in clusters of different cosmic epoch, constraints have also been placed on BCG growth (e.g. Aragon-Salamanca et al. 1998; Collins & Mann 1998; Burke et al. 2000; Nelson et al. 2002). It has been suggested that BCGs in X-ray-luminous clusters seem to evolve passively, with no or little (stellar) mass accretion, while those in less luminous clusters seem to exhibit strong mass accretion, or no evolution in luminosity (e.g. Brough et al. 2002; Nelson et al. 2002, and references therein). We note that using a fixed X-ray luminosity as a cluster mass division is not ideal, because at larger redshifts the same luminosity corresponds to progressively smaller mass. Comparison of BCGs in low X-ray luminosity clusters across a wide range in redshift introduces a mass trend which can explain the inferred strong BCG mass accretion with decreasing redshift. As for X-ray luminous clusters, the resolution may lie in the way the  $L_b$ - $M$  correlation evolves with time.

This also leads to the issue noted in §3.2: if the BCGs of different masses do form a continuum in their evolution, the progenitors of BCGs in present-day high mass clusters are not necessarily the *present-day* low mass cluster BCGs. It is BCGs in low mass clusters at higher redshifts that should be compared to the present-day high mass cluster BCGs. We will investigate this in a future publication.

## 6. SUMMARY

Based on the rich dataset provided by the 2MASS, we systematically examine various cluster properties in the near-IR  $K$ -band for a large sample of 93 clusters and groups (papers I & II). Paper I develops the basic technique. We study the correlation between total galaxy light and cluster binding mass, and the halo occupation distribution in paper II. Here we focus on the extraordinary properties of the brightest cluster galaxies, and their implications for the total cluster light budget and for cluster evolution. The main findings of this paper are summarized as follows:

1. The BCG projected position coincides with the peak in X-ray emission, in agreement with previous findings. In  $\sim 80\%$  of the cases, the BCG location can serve as cluster center to within 10% of the virial radius.
2. The  $K$ -band BCG luminosity shows clear correlation

with cluster mass;  $L_b \propto M^{0.26 \pm 0.04}$  for all clusters in our sample. Combined with a large optically-selected group sample (from the UZC-SSRS2 catalog), we find that the correlation between the BCG luminosity and the cluster mass extends to even lower mass scales.

3. We argue that BCGs likely grow in luminosity via mergers with other luminous galaxies, most likely BCGs from subclusters that have fallen into the cluster. A comparison between the luminosity functions in high and low mass clusters shows a lower density of luminous galaxies ( $\sim L_*$ ) in more massive clusters. The luminosity from these missing galaxies could not make up the differences between the BCG luminosity in high and low mass clusters. On the other hand, based on the luminosity distribution of clusters at different masses, there appear to be enough very luminous galaxies ( $> L_*$ ) in intermediate or low mass clusters to supply the luminosity needed for the BCG growth with increasing cluster mass.

4. The BCG-to-total galaxy light ratio is a decreasing function of cluster mass; at group scales BCG light constitutes roughly half of the total light in galaxies, while in the most massive systems in our sample they only account for 5 – 10% of the light in galaxies. The decreasing importance of BCGs in the overall cluster light budget can be explained if the luminosity growth rates of BCGs (by merging with other luminous galaxies) are slower than the luminosity growth rates of clusters (by accreting isolated galaxies or from smaller clusters that have merged).

5. Second- and third-ranked galaxies show clear trends of increasing galaxy luminosity, but decreasing galaxy-to-cluster light fraction, as a function of cluster mass, as do the BCGs. These similarities suggest that the brightest galaxies share a similar formation and evolution history. At group scales the few brightest galaxies make up almost all the light, while at the other mass extreme the brightest three galaxies only account for 10% of the massive cluster light.

6. We estimate the amount of diffuse light that is present in the intracluster space (which includes any envelope surrounding the BCG) as a function of cluster mass. Two simple models are considered; the first one makes use of the observed total galaxy light-cluster mass relation, as well as the BCG light-cluster mass correlation. The second model takes into account the assembly history of clusters, and uses the observed  $L$ - $M$  relation. Both models suggest that the amount of ICL increases with cluster mass; for clusters more massive than  $10^{14} M_\odot$  the ICL light fraction ranges from 30% to 60%. The model predictions are in reasonable agreement with both direct observations and numerical simulations.

7. The cluster baryon fraction, including the ICL (roughly a 100% increase in cluster stellar mass), is in good agreement with the *WMAP* result (Bennett et al. 2003). The ICL component reduces the discrepancy between the observed value of the cold baryon fraction ( $\sim 16\%$ ) and that found in numerical simulations.

8. The ICL reduces the cluster iron yields by  $\sim 40\%$ , to a value of 3 times solar, still high compared to the solar vicinity. However, with the ICL included, the observations indicate a uniform iron production efficiency for clusters of different masses. Within a simple stellar population model described by a Salpeter IMF, the observed starlight

in galaxies and that implied for the ICL is high enough to explain the high iron abundance in clusters. The ICL also helps in accounting for the production of the observed “iron excess” found in the cool-core clusters.

We acknowledge A. Sanderson for help on obtaining relevant information of BCGs from the NED. We thank A. Finoguenov, A. Gonzalez, P. Ricker, C. Sarazin, F. van den Bosch, and D. Zaritsky for useful discussions and sug-

gestions. We thank an anonymous referee for helpful comments. This work was supported in part by the NASA Long Term Space Astrophysics award NAG 5-11415. This publication makes use of data products from the Two Micron All Sky Survey, which is a joint project of the University of Massachusetts and the IPAC/Caltech, funded by the NASA and the NSF. This research has made use of the NED and BAX.

## REFERENCES

- Aragon-Salamanca, A., Baugh, C. M., & Kauffmann, G. 1998, *MNRAS*, 297, 427
- Arnaboldi, M. 2003, *ArXiv e-prints*, astro-ph/0310143
- Arnaboldi, M., Aguerri, J. A. L., Napolitano, N. R., Gerhard, O., Freeman, K. C., Feldmeier, J., Capaccioli, M., Kudritzki, R. P., & Méndez, R. H. 2002, *AJ*, 123, 760
- Arnaboldi, M., Freeman, K. C., Okamura, S., Yasuda, N., Gerhard, O., Napolitano, N. R., Pannella, M., Ando, H., Doi, M., Furusawa, H., Hamabe, M., Kimura, M., Kajino, T., Komiyama, Y., Miyazaki, S., Nakata, F., Ouchi, M., Sekiguchi, M., Shimasaku, K., & Yagi, M. 2003, *AJ*, 125, 514
- Arnaud, M., Rothenflug, R., Boulade, O., Vigroux, L., & Vangioni-Flam, E. 1992, *A&A*, 254, 49
- Böhringer, H., Matsushita, K., Churazov, E., Finoguenov, A., & Ikebe, Y. 2004, *A&A*, 416, L21
- Baumgartner, W. H., Loewenstein, M., Horner, D. J., & Mushotzky, R. F. 2003, *ApJ*, submitted, astro-ph/0309166
- Beers, T. C. & Geller, M. J. 1983, *ApJ*, 274, 491
- Beers, T. C. & Tonry, J. L. 1986, *ApJ*, 300, 557
- Bennett, C. L., Halpern, M., Hinshaw, G., Jarosik, N., Kogut, A., Limon, M., Meyer, S. S., Page, L., Spergel, D. N., Tucker, G. S., Wollack, E., Wright, E. L., Barnes, C., Greason, M. R., Hill, R. S., Komatsu, E., Nolte, M. R., Odegard, N., Peiris, H. V., Verde, L., & Weiland, J. L. 2003, *ApJS*, 148, 1
- Bernstein, G. M., Nichol, R. C., Tyson, J. A., Ulmer, M. P., & Wittman, D. 1995, *AJ*, 110, 1507
- Borgani, S., Murante, G., Springel, V., Diaferio, A., Dolag, K., Moscardini, L., Tormen, G., Tornatore, L., & Tozzi, P. 2004, *MNRAS*, 348, 1078
- Brough, S., Collins, C. A., Burke, D. J., Mann, R. G., & Lynam, P. D. 2002, *MNRAS*, 329, L53
- Burke, D. J., Collins, C. A., & Mann, R. G. 2000, *ApJ*, 532, L105
- Calcáneo-Roldán, C., Moore, B., Bland-Hawthorn, J., Malin, D., & Sadler, E. M. 2000, *MNRAS*, 314, 324
- Castro-Rodríguez, N., Aguerri, J. A. L., Arnaboldi, M., Gerhard, O., Freeman, K. C., Napolitano, N. R., & Capaccioli, M. 2003, *A&A*, 405, 803
- Collins, C., Brough, S., Burke, D., Mann, R., & Lynam, P. 2003, *Ap&SS*, 285, 51
- Collins, C. A. & Mann, R. G. 1998, *MNRAS*, 297, 128
- Cowie, L. L. & Binney, J. 1977, *ApJ*, 215, 723
- De Grandi, S., Ettori, S., Longhetti, M., & Molendi, S. 2004, *A&A*, 419, 7
- De Grandi, S. & Molendi, S. 2001, *ApJ*, 551, 153
- Dubinski, J. 1998, *ApJ*, 502, 141
- Durrell, P. R., Ciardullo, R., Feldmeier, J. J., Jacoby, G. H., & Sigurdsson, S. 2002, *ApJ*, 570, 119
- Edge, A. C. 1991, *MNRAS*, 250, 103
- Ellis, S. C. & Jones, L. R. 2004, *MNRAS*, 348, 165
- Fabian, A. C. 1994, *ARA&A*, 32, 277
- Fasano, G., Bettoni, D., D’Onofrio, M., Kjærgaard, P., & Moles, M. 2002, *A&A*, 387, 26
- Feldmeier, J., Ciardullo, R., Jacoby, G., & Durrell, P. 2004a, *ApJ*, accepted, astro-ph/0407274
- Feldmeier, J. J., Ciardullo, R., Jacoby, G. H., & Durrell, P. R. 2003a, *ApJS*, 145, 65
- Feldmeier, J. J., Ciardullo, R. B., Jacoby, G. H., Durrell, P. R., & Mihos, J. C. 2003b, *ArXiv e-prints*, astro-ph/0310884
- Feldmeier, J. J., Mihos, J. C., Morrison, H. L., Harding, P., & Kaib, N. 2003c, *ArXiv Astrophysics e-prints*, astro-ph/0303340
- Feldmeier, J. J., Mihos, J. C., Morrison, H. L., Harding, P., Kaib, N., & Dubinski, J. 2004b, *ApJ*, accepted, astro-ph/0403414
- Feldmeier, J. J., Mihos, J. C., Morrison, H. L., Rodney, S. A., & Harding, P. 2002, *ApJ*, 575, 779
- Ferguson, H. C., Tanvir, N. R., & von Hippel, T. 1998, *Nature*, 391, 461
- Finoguenov, A., Burkert, A., & Böhringer, H. 2003, *ApJ*, 594, 136
- Finoguenov, A., David, L. P., & Ponman, T. J. 2000, *ApJ*, 544, 188
- Fisher, D., Franx, M., & Illingworth, G. 1995, *ApJ*, 448, 119
- Gal-Yam, A., Maoz, D., Guhathakurta, P., & Filippenko, A. V. 2003, *AJ*, 125, 1087
- Gnedin, O. Y. 2003, *ApJ*, 589, 752
- Gonzalez, A. H., Zabludoff, A. I., & Zaritsky, D. 2004, *ApJ*, submitted, astro-ph/0406244
- Gonzalez, A. H., Zabludoff, A. I., Zaritsky, D., & Dalcanton, J. J. 2000, *ApJ*, 536, 561
- Graham, A., Lauer, T. R., Colless, M., & Postman, M. 1996, *ApJ*, 465, 534
- Graham, A. W. 2002, *MNRAS*, 334, 859
- Gregg, M. D. & West, M. J. 1998, *Nature*, 396, 549
- Grevesse, N. & Sauval, A. J. 1999, *A&A*, 347, 348
- Gunn, J. E. & Gott, J. R. I. 1972, *ApJ*, 176, 1
- Harris, W. E., Harris, G. L. H., & McLaughlin, D. E. 1998, *AJ*, 115, 1801
- Hausman, M. A. & Ostriker, J. P. 1978, *ApJ*, 224, 320
- Hoessel, J. G. 1980, *ApJ*, 241, 493
- Hoessel, J. G., Gunn, J. E., & Thuan, T. X. 1980, *ApJ*, 241, 486
- Hoessel, J. G. & Schneider, D. P. 1985, *AJ*, 90, 1648
- Jarrett, T. H., Chester, T., Cutri, R., Schneider, S., Skrutskie, M., & Huchra, J. P. 2000, *AJ*, 119, 2498
- Jones, C. & Forman, W. 1984, *ApJ*, 276, 38
- Jones, L. R., Ponman, T. J., & Forbes, D. A. 2000, *MNRAS*, 312, 139
- Jones, L. R., Ponman, T. J., Horton, A., Babul, A., Ebeling, H., & Burke, D. J. 2003, *MNRAS*, 343, 627
- Jordán, A., West, M. J., Côté, P., & Marzke, R. O. 2003, *AJ*, 125, 1642
- Karachentsev, I. D., Dolphin, A. E., Geisler, D., Grebel, E. K., Guhathakurta, P., Hodge, P. W., Karachentseva, V. E., Sarajedini, A., Seitzer, P., & Sharina, M. E. 2002, *A&A*, 383, 125
- Katayama, H., Hayashida, K., Takahara, F., & Fujita, Y. 2003, *ApJ*, 585, 687
- Klypin, A., Gottlöber, S., Kravtsov, A. V., & Khokhlov, A. M. 1999, *ApJ*, 516, 530
- Kochanek, C. S., Pahre, M. A., Falco, E. E., Huchra, J. P., Mader, J., Jarrett, T. H., Chester, T., Cutri, R., & Schneider, S. E. 2001, *ApJ*, 560, 566
- Kravtsov, A. V., Berlind, A. A., Wechsler, R. H., Klypin, A. A., Gottlöber, S., Allgood, B., & Primack, J. R. 2004, *ApJ*, 609, 35
- Kroupa, P. 2002, *Science*, Volume 295, Issue 5552, pp. 82-91 (2002), 295, 82
- Lauer, T. R. 1988, *ApJ*, 325, 49
- Lazzati, D. & Chincarini, G. 1998, *A&A*, 339, 52
- Lin, Y.-T., Mohr, J. J., & Stanford, S. A. 2003, *ApJ*, 591, 749
- , 2004, *ApJ*, 610, 745
- Loewenstein, M. 2001, *ApJ*, 557, 573
- Loewenstein, M. & Mushotzky, R. F. 1996, *ApJ*, 466, 695
- Mahdavi, A., Böhringer, H., Geller, M. J., & Ramella, M. 2000, *ApJ*, 534, 114
- Malumuth, E. M. & Richstone, D. O. 1984, *ApJ*, 276, 413
- Merritt, D. 1983, *ApJ*, 264, 24
- , 1984, *ApJ*, 276, 26
- , 1985, *ApJ*, 289, 18
- Mohr, J. J., Evrard, A. E., Fabricant, D. G., & Geller, M. J. 1995, *ApJ*, 447, 8
- Mohr, J. J., Mathiesen, B., & Evrard, A. E. 1999, *ApJ*, 517, 627
- Moore, B., Katz, N., Lake, G., Dressler, A., & Oemler, A. 1996, *Nature*, 379, 613
- Moore, B., Lake, G., & Katz, N. 1998, *ApJ*, 495, 139
- Murante, G., Arnaboldi, M., Gerhard, O., Borgani, S., Cheng, L. M., Diaferio, A., Dolag, K., Moscardini, L., Tormen, G., Tornatore, L., & Tozzi, P. 2004, *ApJ*, 607, L83
- Napolitano, N. R., Pannella, M., Arnaboldi, M., Gerhard, O., Aguerri, J. A. L., Freeman, K. C., Capaccioli, M., Ghigna, S., Governato, F., Quinn, T., & Stadel, J. 2003, *ApJ*, 594, 172
- Navarro, J. F., Frenk, C. S., & White, S. D. M. 1997, *ApJ*, 490, 493
- Nelson, A. E., Gonzalez, A. H., Zaritsky, D., & Dalcanton, J. J. 2002, *ApJ*, 566, 103

- Nipoti, C., Stiavelli, M., Ciotti, L., Treu, T., & Rosati, P. 2003, *MNRAS*, 344, 748
- Oegerle, W. R. & Hill, J. M. 2001, *AJ*, 122, 2858
- Oemler, A. 1976, *ApJ*, 209, 693
- Okamura, S., Yasuda, N., Arnaboldi, M., Freeman, K. C., Ando, H., Doi, M., Furusawa, H., Gerhard, O., Hamabe, M., Kimura, M., Kajino, T., Komiyama, Y., Miyazaki, S., Nakata, F., Napolitano, N. R., Ouchi, M., Pannella, M., Sekiguchi, M., Shimasaku, K., & Yagi, M. 2002, *PASJ*, 54, 883
- Ostriker, J. P. & Tremaine, S. D. 1975, *ApJ*, 202, L113
- Peterson, J. R., Paerels, F. B. S., Kaastra, J. S., Arnaud, M., Reiprich, T. H., Fabian, A. C., Mushotzky, R. F., Jernigan, J. G., & Sakelliou, I. 2001, *A&A*, 365, L104
- Portinari, L., Moretti, A., Chiosi, C., & Sommer-Larsen, J. 2004, *ApJ*, 604, 579
- Postman, M. & Lauer, T. R. 1995, *ApJ*, 440, 28
- Quintana, H. & Lawrie, D. G. 1982, *AJ*, 87, 1
- Quintana, H., Ramirez, A., & Way, M. J. 1996, *AJ*, 111, 603
- Ramella, M., Geller, M. J., Pisani, A., & da Costa, L. N. 2002, *AJ*, 123, 2976
- Renzini, A., Ciotti, L., D’Ercole, A., & Pellegrini, S. 1993, *ApJ*, 419, 52
- Rhee, G. F. R. N. & Latour, H. J. 1991, *A&A*, 243, 38
- Richstone, D. O. 1976, *ApJ*, 204, 642
- Rines, K., Geller, M. J., Diaferio, A., Kurtz, M. J., & Jarrett, T. H. 2004, *AJ*, submitted, astro-ph/0402242
- Salpeter, E. E. 1955, *ApJ*, 121, 161
- Sandage, A. 1972, *ApJ*, 178, 1
- . 1976, *ApJ*, 205, 6
- Sandage, A. & Hardy, E. 1973, *ApJ*, 183, 743
- Schechter, P. 1976, *ApJ*, 203, 297
- Scheick, X. & Kuhn, J. R. 1994, *ApJ*, 423, 566
- Schneider, D. P., Gunn, J. E., & Hoessel, J. G. 1983a, *ApJ*, 264, 337
- . 1983b, *ApJ*, 268, 476
- Schombert, J. M. 1986, *ApJS*, 60, 603
- . 1987, *ApJS*, 64, 643
- . 1988, *ApJ*, 328, 475
- Sheth, R. K. & Tormen, G. 1999, *MNRAS*, 308, 119
- Somerville, R. S. & Kolatt, T. S. 1999, *MNRAS*, 305, 1
- Sommer-Larsen, J., Romeo, A. D., & Portinari, L. 2004, *MNRAS*, submitted, astro-ph/0403282
- Struble, M. F. & Rood, H. J. 1999, *ApJS*, 125, 35
- Thuan, T. X. & Kormendy, J. 1977, *PASP*, 89, 466
- Tonry, J. L. 1987, in *IAU Symp. 127: Structure and Dynamics of Elliptical Galaxies*, 89–96
- Tremaine, S. 1990, in *Dynamics and interactions of galaxies*, 394–405
- Trentham, N. & Mobasher, B. 1998, *MNRAS*, 293, 53
- Treu, T., Ellis, R. S., Kneib, J., Dressler, A., Smail, I., Czoske, O., Oemler, A., & Natarajan, P. 2003, *ApJ*, 591, 53
- Tyson, J. A. & Fischer, P. 1995, *ApJ*, 446, L55
- Tyson, J. A., Kochanski, G. P., & dell’Antonio, I. P. 1998, *ApJ*, 498, L107
- Uson, J. M., Boughn, S. P., & Kuhn, J. R. 1991, *ApJ*, 369, 46
- Vilchez-Gomez, R., Pello, R., & Sanahuja, B. 1994, *A&A*, 283, 37
- Weil, M. L. & Hernquist, L. 1996, *ApJ*, 460, 101
- Welch, G. A. & Sastry, G. N. 1971, *ApJ*, 169, L3
- West, M. J. 1994, *MNRAS*, 268, 79
- White, P. M., Bothun, G., Guerrero, M. A., West, M. J., & Barkhouse, W. A. 2003, *ApJ*, 585, 739
- Willman, B., Governato, F., Wadsley, J., & Quinn, T. 2004, *MNRAS*, submitted, astro-ph/0405094
- Wu, X., Xue, Y., & Fang, L. 1999, *ApJ*, 524, 22
- Yamada, T., Koyama, Y., Nakata, F., Kajisawa, M., Tanaka, I., Kodama, T., Okamura, S., & De Propriis, R. 2002, *ApJ*, 577, L89
- Zabludoff, A. I., Huchra, J. P., & Geller, M. J. 1990, *ApJS*, 74, 1
- Zaritsky, D., Gonzalez, A. H., & Zabludoff, A. I. 2004, *ApJ*, submitted, astro-ph/0406291
- Zibetti, S. & White, S. D. M. 2004, *ArXiv Astrophysics e-prints*, astro-ph/0404326
- Zwicky, F. 1951, *PASP*, 63, 61